Journal of Medicinal Chemistry

Article

Cite This: J. Med. Chem. XXXX, XXX, XXX−XXX

pubs.acs.org/jmc

Discovery of QCA570 as an Exceptionally Potent and Efficacious Proteolysis Targeting Chimera (PROTAC) Degrader of the Bromodomain and Extra-Terminal (BET) Proteins Capable of Inducing Complete and Durable Tumor Regression

Chong Qin,[†,‡,◆] Yang Hu,[†,‡,◆] Bing Zhou,[†,‡,○,◆] Ester Fernandez-Salas,[†,⊥,◆] Chao-Yie Yang,[†,‡] Liu Liu,[†,‡] Donna McEachern,[†,‡] Sally Przybranowski,[†,‡] Mi Wang,[†,‡] Jeanne Stuckey,[#] Jennifer Meagher,[#] Longchuan Bai,[†,‡] Zhuo Chen,[†,‡] Mei Lin,[†,‡] Jiuling Yang,[†,‡,§] Danya N. Ziazadeh,[†,‡] Fuming Xu,[†,‡] Jiantao Hu,[†,‡] Weiguo Xing,[†,‡] Liyue Huang,[†,‡] Siwei Li,[▽] Bo Wen,[▽] Duxin Sun,[▽] and Shaomeng Wang*[,†,‡,§,∥]

[†]The Rogel Cancer Center and [‡]Departments of Internal Medicine, [§]Pharmacology, [∥]Medicinal Chemistry, and [⊥]Pathology, University of Michigan Medical School, Ann Arbor, Michigan 48109, United States

[#]Life Sciences Institute and [▽]Pharmacokinetics Core, College of Pharmacy, University of Michigan, Ann Arbor, Michigan 48109, United States

Supporting Information

ABSTRACT: Proteins of the bromodomain and extra-terminal (BET) family are epigenetics "readers" and promising therapeutic targets for cancer and other human diseases. We describe herein a structure-guided design of [1,4]oxazepines as a new class of BET inhibitors and our subsequent design, synthesis, and evaluation of proteolysis-targeting chimeric (PROTAC) small-molecule BET degraders. Our efforts have led to the discovery of extremely potent BET degraders, exemplified by QCA570, which effectively induces degradation of BET proteins and inhibits cell growth in human acute leukemia cell lines even at low picomolar concentrations. QCA570 achieves complete and durable tumor regression in leukemia xenograft models in mice at well-tolerated dose-schedules. QCA570 is the most potent and efficacious BET degrader reported to date.

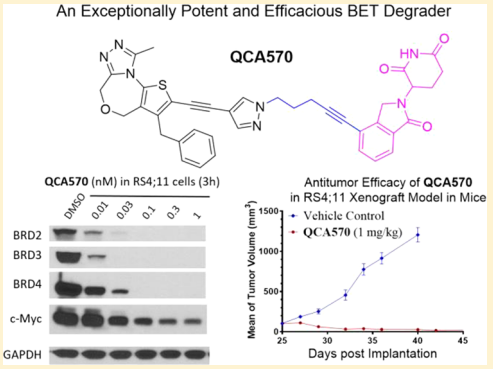

INTRODUCTION

Bromodomain-containing proteins function as epigenetic "readers".[1−3] Among them, the bromodomain and extra-terminal (BET) family of proteins, which includes BRD2, BRD3, BRD4, and testis-specific BRDT, have emerged as therapeutic targets for cancer, inflammation, HIV infection, CNS disorders, cardiovascular diseases, and male contraception.[4−10]

All the members of the BET protein family contain two bromodomains (BD1 and BD2) that bind the acetylated lysine residues in histone tails and thus regulate gene transcription. In recent years, potent and specific small-molecule BET inhibitors such as JQ-1,[11] I-BET762 (GSK525762A),[12] and I-BET151,[13] which bind to these bromodomains, have been discovered.[14−27] A number of BET inhibitors, including I-BET762 (GSK525762),[12] OTX-015 (MK-8628),[28] and TEN-010 (RO6870810),[29] have advanced into clinical development as a new class of therapeutics for the treatment of human cancers.

The proteolysis targeting chimera (PROTAC) concept was formally proposed by Deshaies and Crews in 2001,[30] and the PROTAC strategy has recently gained attention for its promise in the discovery and development of completely new classes of small-molecule therapeutics.[31−48] PROTAC degrader molecules are designed to contain a ligand for the target protein of interest tethered to a linker, which is attached to a second ligand capable of binding to and recruiting an E3 ligase complex to ubiquitinate and degrade the target protein. A number of laboratories, including ours, have employed the PROTAC strategy for the design of small-molecule degraders of BET proteins.[43−45,47−49] Recently, we reported the discovery of ZBC246 and ZBC260 as highly potent PROTAC BET degraders that are capable of inducing complete degradation of BET proteins in breast cancer and leukemia cells at low to subnanomolar concentrations.[44,45] ZBC246 and ZBC260 are >100-times more potent than the corresponding BET inhibitors in the inhibition of cell growth in the majority of leukemia and breast cancer cell lines evaluated.[44,45] These two BET degraders are also very effective in inhibition of tumor growth in breast cancer xenograft models,[44,45] and ZBC260 induces tumor regression in acute leukemia xenograft models in mice. Our data

Received: March 30, 2018

DOI: 10.1021/acs.jmedchem.8b00506
J. Med. Chem. XXXX, XXX, XXX−XXX

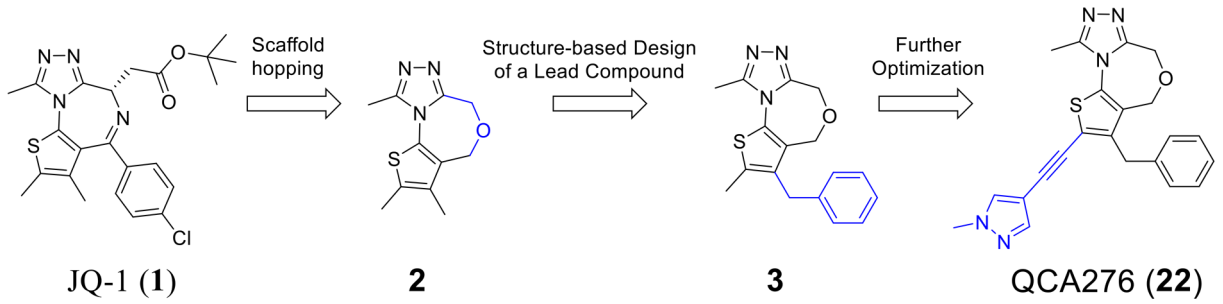

Figure 1. Scaffold hopping and structure-based design of [1,4]oxazepines as a new class of BET inhibitors.

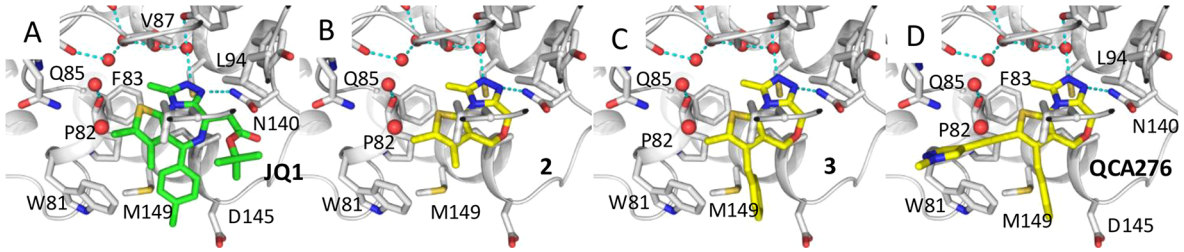

Figure 2. (A) Previously published cocrystal structure of (+)-JQ-1 in complex with the BRD4 BD1 domain protein (PDB ID: 3MXF). (B–D) Predicted binding models of compounds **2**, **3**, and **22** (QCA276) in a complex with BRD4 BD1. Hydrogen bonds are depicted by cyan dashed lines. Water molecules are shown as red spheres.

on ZBC246 and ZBC260 suggest that PROTAC BET degraders may have a promising therapeutic potential for the treatment of leukemia and solid tumors.

In the present study, we describe the design, synthesis, and evaluation of novel PROTAC BET degraders based upon a new class of BET inhibitors that we have designed. Our efforts have yielded the discovery of QCA570 as an extremely potent and highly efficacious BET degrader, capable of degrading BET proteins at low picomolar (pM) concentrations in leukemia cells and achieving complete and durable tumor regression in mice at well-tolerated dose-schedules. QCA570 is the most potent and efficacious BET degrader reported to date.

RESULTS AND DISCUSSION

Structure-Guided Design of 1,4-Oxazepines as a New Class of BET Inhibitors. Our goal was to discover new classes of BET inhibitors that target BET bromodomains and then use them to design novel BET degraders with improved potency and efficacy.

Since BRD4 BD1 domain, but not BRD4 BD2 domain, has been shown to regulate gene expression,[50] we focused our design on new classes of BET inhibitors to target the BRD4 BD1 domain. Our modeling showed that 2,9-dimethyl-4*H*,6*H*-thieno[2,3-*e*][1,2,4]triazolo[3,4-*c*][1,4]oxazepine (**2**, Figure 1) can closely mimic the 2,3,4,9-tetramethyl-6*H*-thieno[3,2-*f*]-[1,2,4]triazolo[4,3-*a*][1,4]diazepine core in JQ-1 when interacting with the BRD4 BD1 domain protein (Figure 2). We synthesized compound **2** and determined that it binds to BRD4 BD1 protein with a K_i value of 1.5 μM (Table 1) in our fluorescence polarization (FP) assay.[26,27]

The *p*-chlorophenyl group in JQ-1 is critical for the high binding affinity of JQ-1 to the BRD4 BD1 protein through its interaction with the Trp-Pro-Phe (WPF) shelf in BRD4 BD1, but compound **2** lacks the corresponding *p*-chlorophenyl group present in JQ-1 (Figure 1). To capture the interactions of the *p*-chlorophenyl group in JQ-1 with BRD4, we modeled compounds with a substituent at the 3-position of the thiophene in compound **2**. Modeling suggested that a benzyl group, but not a phenyl group, at the 3-position of the thiophene could effectively interact with the WPF shelf in BRD4, and this led to the design of compound **3** (Figure 1). Our FP assay showed that compound **3** binds to BRD4 BD1 protein with a K_i value of 33 nM (Table 1) and is therefore >40-times more potent than **2**.

In the cocrystal structure of JQ-1 complexed with BDR4 BD1 protein,[10,11] the 2-methyl group on the thiophene group enjoys van der Waals interactions with the Trp81, Gln85, and Leu92 residues in the protein. Accordingly, we performed further modification of **3** to improve its binding affinity to the protein. To assess the contribution of the corresponding methyl group in compound **3** to the BRD4 BD1 binding, we eliminated this methyl group, producing compound **4**. In our FP binding assay, compound **4** has a K_i value of 820 nM to the protein and is thus 25-times less potent than compound **3** (Table 1). The significant reduction in binding affinity of compound **4** to the protein when compared to compound **3** clearly reveals the important contribution of this methyl group to the binding affinity and suggests that further modifications of the methyl group in **3** may improve the binding affinity to BRD4.

Analysis of the cocrystal structure of JQ-1 in a complex with BRD4 BD1[10,11] and our modeled structure of compound **3** in a complex with BRD4 BD1 (Figure 2) showed that there is a channel formed by Trp81, Pro82, Gln85, Asp88, Lys91, and Leu92, which is adjacent to the methyl group on the thiophene. We explored this channel by further modification of the methyl group in compound **3**.

Replacement of the methyl group in **3** with a hydrophobic and bulkier isopropyl group yielded compound **5**, which is >50-times less potent than **3** in binding to BRD4 BD1. Replacement of the methyl by a 4-tetrahydro-2*H*-pyran group generated compound **6**, which is also >50-times less potent than **3** in binding to BRD4 BD1 (Table 1). The reduced binding affinities of **5** and **6** to BRD4 BD1 when compared to that of **3** are consistent with our modeling analysis, which showed that the channel around the methyl group is fairly narrow and cannot accommodate groups

DOI: 10.1021/acs.jmedchem.8b00506
J. Med. Chem. XXXX, XXX, XXX−XXX

Table 1. Binding Affinities of Our Newly Designed BET Inhibitors and Reference Compounds (+)-JQ-1 and OTX-015 to BRD4 BD1 Protein, As Determined in Our FP-Based Binding Assay

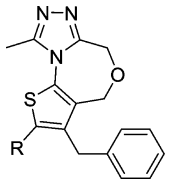

Compound	R	BRD4 BD1	
		IC_{50}(nM)	K_i(nM)
1 (JQ-1)		22 ± 3	5.3 ± 1.0
2		4400 ± 700	1500 ± 200
3	CH_3	100 ± 10	33 ± 4
4	-H	2300 ± 600	820 ± 210
5	-isopropyl	9400 ± 600	3300 ± 200
6	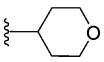	8100 ± 700	2800 ± 300
7	-cyclopropyl	550 ± 110	190 ± 40
8		210 ± 10	70 ± 1
9		720 ± 60	250 ± 20
10	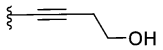	45 ± 4	13 ± 1
11	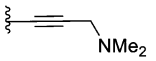	270 ± 10	92 ± 2
12	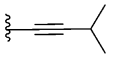	44 ± 3	13 ± 1
13	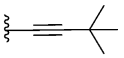	200 ± 90	68 ± 10
14	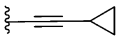	18 ± 2	3.7 ± 0.7
15	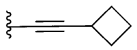	34 ± 3	9.5 ± 1.1
16	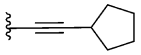	63 ± 10	20 ± 3
17	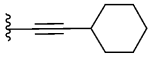	200 ± 24	66 ± 9
18	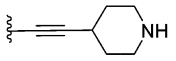	200 ± 9	68 ± 3
19	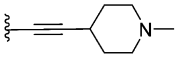	86 ± 11	28 ± 4
20	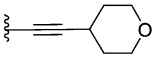	34 ± 2	9.6 ± 0.9
21	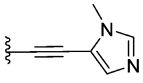	50 ± 9	15 ± 3
22 (QCA276)	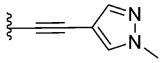	10 ± 3	2.3 ± 1.0
23	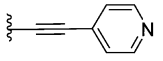	14 ± 5	4.2 ± 0.8
24	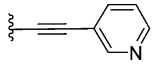	11 ± 1	2.1 ± 0.3
25	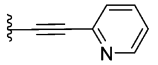	13 ± 4	2.7 ± 1.2
OTX-015		23 ± 1	5.7 ± 0.5

DOI: 10.1021/acs.jmedchem.8b00506
J. Med. Chem. XXXX, XXX, XXX−XXX

Table 2. Binding Affinities of 22 (QCA276) to Recombinant Human BRD2, BRD3, and BRD4 BD1 and BD2 Proteins As Determined in Our FP-Based Assays

	BRD2		BRD3		BRD4	
	BD1	BD2	BD1	BD2	BD1	BD2
IC_{50} (nM)	3.5 ± 0.3	40.6 ± 4.6	16.4 ± 2.8	35.1 ± 8.2	10.7 ± 2.8	66.6 ± 11.2
K_i (nM)	1.7 ± 0.1	8.5 ± 0.8	2.5 ± 0.9	6.5 ± 0.9	2.3 ± 1.0	18.5 ± 5.2

Table 3. Chemical Structures of Designed PROTAC BET Degraders and Their IC_{50} Values in Inhibition of Cell Growth in Three Acute Leukemia Cell Lines MV4;11, MOLM13, and RS4;11[a]

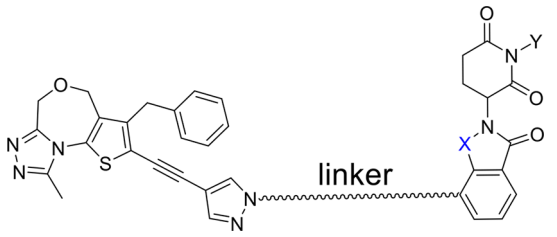

Compound	linker	X	Y	IC_{50} (nM) in cell growth inhibition		
				MV4;11	MOLM13	RS4;11
22 (BET inhibitor)				55.8 ± 7.5	207 ± 20	173 ± 20
26		CO	H	>1000	>1000	>1000
27		CO	H	19.7 ± 0.76	311	20.8 ±1.4
28	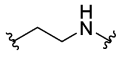	CO	H	0.47 ± 0.11	2.23 ± 0.52	0.379 ± 0.037
29	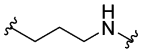	CO	H	0.138 ± 0.008	0.56 ± 0.1	0.038 ± 0.005
30	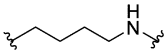	CO	H	0.0654 ± 0.007	0.19 ± 0.02	0.02 ± 0.01
31	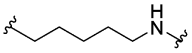	CO	H	0.092 ± 0.007	0.19 ± 0.02	0.02 ± 0.01
32	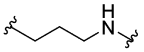	CH_2	H	0.035 ± 0.007	0.51 ± 0.09	0.025 ± 0.004
33	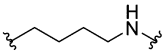	CH_2	H	0.051 ± 0.004	0.18 ± 0.02	0.0012 ± 0.0001
34	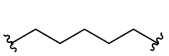	CH_2	H	0.14 ± 0.01	0.53 ± 0.18	0.081 ± 0.009
35 (QCA570)	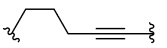	CH_2	H	0.0083 ± 0.0012	0.062 ± 0.009	0.032 ± 0.003
36	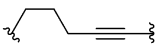	CO	H	0.72 ± 0.09	1.6 ± 0.3	0.39 ± 0.02
37	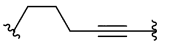	CH_2	Me	25.8 ± 4.4	183 ± 25	43.7 ± 5.2
dBET1				42 ± 14	140 ± 28	79 ± 12
ARV-825				1.05 ± 0.30	18.2 ± 4.0	3.3 ± 0.7
ARV-771				0.43 ± 0.12	7.45 ± 1.45	2.4 ± 0.7
ZBC260 (BETd-260)				0.36 ± 0.28	2.2 ± 0.2	0.051 ± 0.018

[a]Cells were treated with compounds for 96 h, and viability was assessed with a Cell Counting Kit-8 (CCK-8) assay.

much bulkier than the methyl group. We therefore decided to focus on groups smaller than isopropyl or 4-tetrahydro-2*H*-pyran.

Replacement of the methyl by cyclopropyl gave compound **7**, which is >10-times more potent than **5** but still >5-times less potent than **3** in binding to BRD4 BD1 protein. Next, we replaced the methyl group with a linear ethynyl group, producing compound **8**. Compound **8** binds to BRD4 BD1 with a K_i value of 70 nM and is therefore two times less potent than compound **3**. Changing the ethynyl group to nitrile, a linear and polar group, yielded compound **9**, which is three times less potent than **8** or six times less potent than **3** (Table 1).

The ethynyl group in compound **8** provided us with an opportunity to further explore this channel in BRD4 BD1. Addition of a hydroxyethyl to the ethynyl group gave compound **10**, which is two times more potent than **3**. Replacing the

DOI: 10.1021/acs.jmedchem.8b00506
J. Med. Chem. XXXX, XXX, XXX−XXX

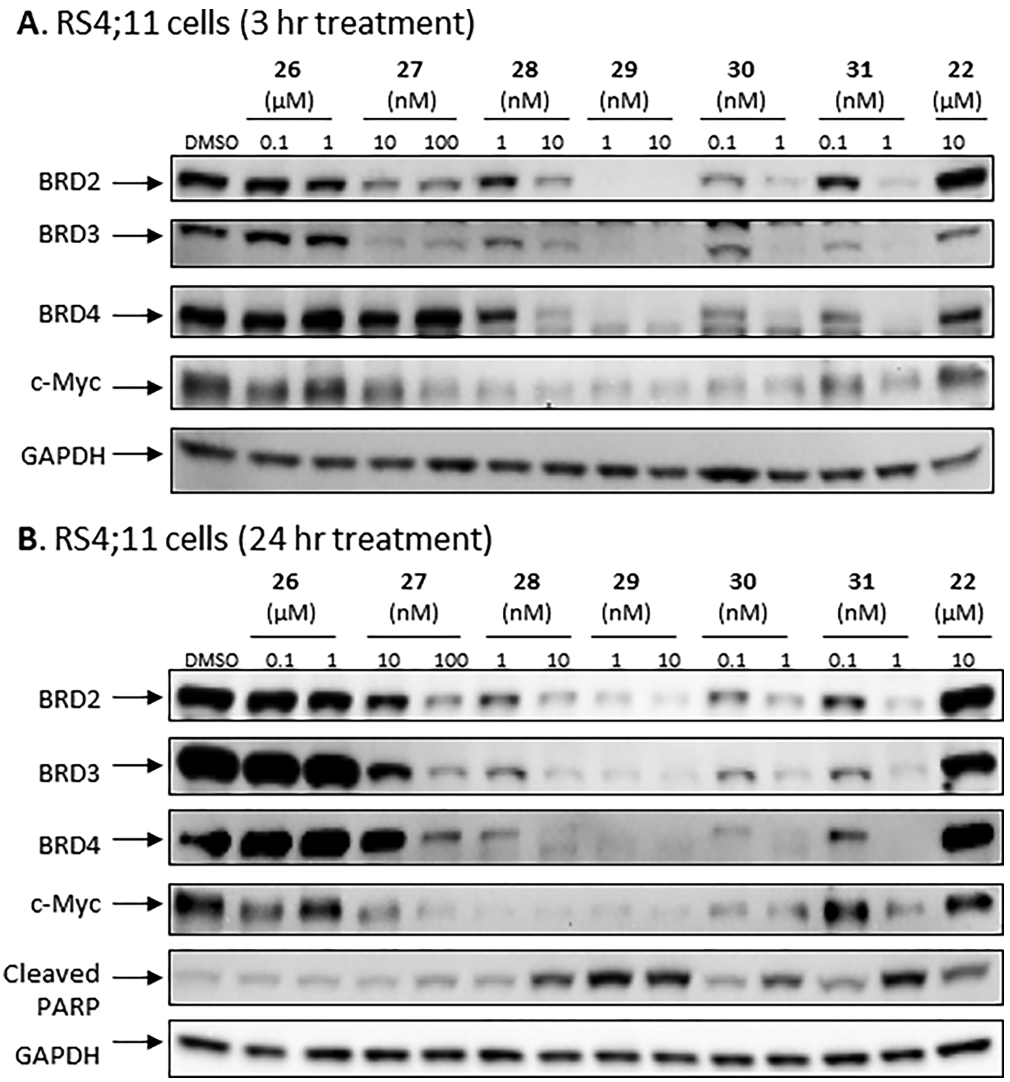

Figure 3. Western blotting analysis of BRD2, BRD3, and BRD4 proteins in RS4;11 cells treated with BET inhibitor **22** (QCA276), **26**, and BET degraders **27**, **28**, **29**, **30**, and **31**. RS4;11 cells were treated for 3 h (A) or 24 h (B) with each individual compound at the indicated concentrations. BRD2, BRD3, and BRD4 proteins, c-Myc, and cleaved PARP were probed by Western blot with specific antibodies, and GAPDH was used as the loading control.

$-CH_2OH$ in **10** with a dimethylamino group gave compound **11**, which has a K_i value of 92 nM and thus a potency similar to that of **3**. We synthesized compounds with additional hydrophobic substituents, such as isopropyl, *t*-butyl, cyclopropyl, cyclobutyl, cyclopentyl, and cyclohexyl groups on the ethynyl group, yielding **12**, **13**, **14**, **15**, **16**, and **17**, respectively (Table 1). Among these compounds, **14** has a K_i value of 3.7 nM and is thus 10 times more potent than **3**.

We next synthesized **18** containing a piperidine substituent, **19** containing a methylpiperidine substituent, and **20** containing a tetrahydropyran substituent on the ethynyl group. Compounds **18**, **19**, and **20** bind to BRD4 BD1 with K_i values of 68, 28, and 9.6 nM, respectively. The binding affinities of **19** and **20** are stronger than that of **17**, and this shows that a polar atom at the tip of the cyclohexyl substituent in **17** is tolerated well.

Several compounds containing a heteroaromatic substituent on the ethynyl group were synthesized, including **21** containing a 1-methyl-1*H*-imidazole, **22** (QCA276) containing a 1-methyl-1*H*-pyrazole, and **23**, **24**, and **25** each containing a pyridine ring in different orientations. With the exception of **21**, which has a K_i value of 15 nM, compounds **22**–**25** all have K_i values to BRD4 BD1 protein below 14 nM (Table 1). In our binding assay, OTX-015 has a K_i value of 5.7 nM to BRD4 BD1 protein and compounds **22**–**25** are thus equally potent binders to BRD4 BD1, as compared to OTX-015.

We further evaluated compound **22** for its binding affinities to BRD4 BD2, and BRD2–3 BD1, and BD2 proteins in our FP assays,[24] and the data are presented in Table 2. Compound **22** binds to BRD2 BD1 and BRD3 BD1 with K_i values of 1.7 and 2.5 nM, respectively. It also binds to BRD2 BD2, BRD3 BD2, and BRD4 BD2 with high binding affinities, giving K_i values of 8.5, 6.5, and 18.5 nM, respectively. Accordingly, compound **22** was selected as the lead BET inhibitor in our subsequent design of a new class of PROTAC BET degraders, described below.

Design of a New Class of PROTAC BET Degraders Based upon the BET Inhibitor 22 (QCA-276). Our modeling of **22** (QCA-276) complexed with BRD4 BD1 protein suggested that the 1-methyl-1*H*-pyrazole group is exposed to the solvent environment, making it a suitable site at which to anchor a chemical link to a ligand for an E3 ligase complex for the design of PROTAC BET degraders.

DOI: 10.1021/acs.jmedchem.8b00506
J. Med. Chem. XXXX, XXX, XXX–XXX

Cereblon is an adaptor protein for the cullin 4A RING E3 ligase complex,[51] and thalidomide[51,52] and lenalidomide[53] are known to be cereblon ligands. In our previous studies, we successfully employed thalidomide and lenalidomide in our design of potent and efficacious BET degraders ZBC246 and ZBC260.[44,45] We hence chose to employ thalidomide and lenalidomide as the ligands for cereblon/cullin 4A and compound **22** as the BET inhibitor for the design of new PROTAC BET degraders.

We first synthesized compounds **26**−**31** as potential BET degraders, by linking one of the nitrogen atoms in the pyrazole group of **22** to the C4 atom of the isoindoline ring in thalidomide (Table 3). As shown in our earlier study,[44] the MV4;11, RS4;11, and MOLM-13 acute leukemia cell lines are very responsive to both BET inhibitors and degraders, and accordingly, we evaluated our newly synthesized BET degraders for their activity in the inhibition of cell growth in these three acute leukemia cell lines, and the data obtained are summarized in Table 3. As a control, we also evaluated the BET inhibitor **22** for its inhibition of cell growth in these leukemia cell lines.

Consistent with its high binding affinities to BET proteins, the BET inhibitor (**22**) is an effective inhibitor of cell growth, with IC_{50} values of 55.8, 207, and 173 nM in the MV4;11, MOLM-13, and RS4;11 cell lines, respectively (Table 3).

The potential BET degrader (**26**), in which the pyrazole group in the BET inhibitor portion is directly linked to thalidomide, failed to show significant cell growth inhibitory activity at concentrations up to 1000 nM in any of these three leukemia cell lines (Table 3). Western blotting analysis consistently showed that at concentrations up to 1000 nM, compound **26** failed to induce degradation of BRD2, BRD3, and BRD4 proteins in the RS4;11 cells even after a 24 h treatment (Figures 3 and S1).

Compound **27**, which possesses a $-CH_2O-$ linker between the pyrazole group in the BET inhibitor portion and the thalidomide, achieves IC_{50} values of 19.7, 311, and 20.8 nM in the MV4;11, MOLM-13, and RS4;11 cell lines, respectively (Table 3). In contrast to **26**, Western blotting showed that **27**, at concentrations as low as 10 nM, is very effective in inducing degradation of BRD2, BRD3, and BRD4 proteins in the RS4;11 cells in a time- and dose-dependent manner (Figures 3 and S1). Interestingly, **27** induces degradation of BRD2 and BRD3 proteins more effectively than the BRD4 protein (Figures 3 and S1).

Our previous study showed that the nature of the PROTAC linker between the BET inhibitor portion and thalidomide plays a key role in the potency of a BET degrader in degrading BET proteins and therefore in inhibition of cell growth.[44] Accordingly, we synthesized and evaluated a number of BET degraders with linkers longer than that in **27**. Compound **28** containing a $-(CH_2)_2NH-$ linker is a highly potent BET degrader, achieving IC_{50} values of 0.47, 2.2, and 0.38 nM in cell growth inhibition in MV4;11, MOLM-13, and RS4;11 cell lines, respectively (Table 3). Thus, **28** is >50-times more potent than **27** in each of these three cell lines.

Increasing the linker length in **28** by one additional methylene yielded **29**, which shows further improved potency in cell growth inhibition in each of these three cell lines. Compound **29** achieves IC_{50} values of 0.14, 0.56, and 0.038 nM in cell growth inhibition in MV4;11, MOLM-13, and RS4;11 cell lines, respectively, and is therefore 3−10 times more potent than **28**.

Increasing the linker length in **29** by an additional methylene led to **30**, which is 2−3 times more potent than **29** in cell growth inhibition in each of the three leukemia cell lines. However, a further increase in the linker length in **30** by one more methylene group, resulting in, for example, **31**, fails to improve the potency in cell growth inhibition in any of the three cell lines. Compounds **30** and **31** in fact have very similar potencies in all three cell lines, with the data indicating that the linker in **30** is optimal. Indeed, compound **30** achieves extremely high potencies in all three leukemia cell lines with IC_{50} values of 0.065, 0.19, and 0.02 nM in inhibition of cell growth (Table 3).

We evaluated compounds **27**−**31** for their ability to induce degradation of BET proteins in the RS4;11 cells (Figures 3 and S1). Our Western blotting data showed that **29**, and especially **30** and **31** are extremely potent inducers of degradation of BET proteins and are in fact very effective at concentrations as low as 0.1 nM after a 3 h treatment. Consistent with their reduced potencies in inhibition of cell growth in the RS4;11 cell line, compounds **27** and **28** are much less potent than compounds **29**, **30**, and **31** in inducing degradation of BET proteins.

Since c-Myc protein expression is regulated by BET proteins,[54] we evaluated the effect of our BET degraders on c-Myc. Consistent with their high potency in inducing complete degradation of BET proteins, the potent BET degraders **30** and **31** are also very effective in reducing the levels of c-Myc protein in the RS4;11 cells (Figures 3 and S1). For example, both **30** and **31** reduce the levels of c-Myc protein in a 3 h treatment time at concentrations as low as 0.1 nM (Figure 3A). These data further confirm that **30** and **31** are highly potent BET degraders. Moreover, compounds **28**, **29**, **30**, and **31** all potently induce apoptosis at 1 and 10 nM after a 24 h treatment as revealed by cleavage of PARP (Figure 3B), while the inhibitor **22** at 10 μM induces PARP cleavage only marginally.

We next synthesized **32** and **33** by converting the 3-carbonyl group in the thalidomide moiety of **29** and **30** to a methylene group in an effort to further improve potency. Both **32** and **33** have IC_{50} values in the low picomolar to subnanomolar range in cell growth inhibition in these leukemia cell lines and are therefore highly potent BET degraders (Table 3).

To further examine the effect of the linking group, we synthesized and evaluated compounds **34** and **35**. Changing the NH linking group in **33** to a methylene group yielded **34**, which has picomolar IC_{50} values in inhibition of cell growth in each of the three leukemia cell lines. Replacing the $NHCH_2$ linker in **33** with an ethynyl group gave **35** (QCA570), which inhibits cell growth in MV4;11, MOLM-13, and RS4;11 cell lines with IC_{50} values of 8.3, 62, and 32 pM, respectively (Table 3). Converting the 3-carbonyl group in the thalidomide moiety to a methylene group gave **36**, which is 10−100 times less potent than **35**.

The amino group of the piperidine-2,6-dione in thalidomide and lenalidomide forms a strong hydrogen bond with cereblon, which is revealed in the cocrystal structures.[52,53] Consistently, methylation of the amino group of the piperidine-2,6-dione in thalidomide and lenalidomide completely abolishes their binding to cereblon.[37] To facilitate our mechanistic investigations for this class of BET degraders, we synthesized compound **37**, in which the amino group of the piperidine-2,6-dione in **35** is methylated. Compound **37** is a fairly potent inhibitor of cell growth in all three leukemia cell lines, but it is >10,000-times less potent than **35** in each of these three leukemia cell lines, supporting that the high potency of **35** as a BET degrader is dependent on binding to cereblon. Compound **37** and the corresponding BET inhibitor **22** have similar IC_{50} values in inhibition of cell growth in the MV4;11, MOLM-13, and RS4;11 cell lines (Table 3).

DOI: 10.1021/acs.jmedchem.8b00506
J. Med. Chem. XXXX, XXX, XXX−XXX

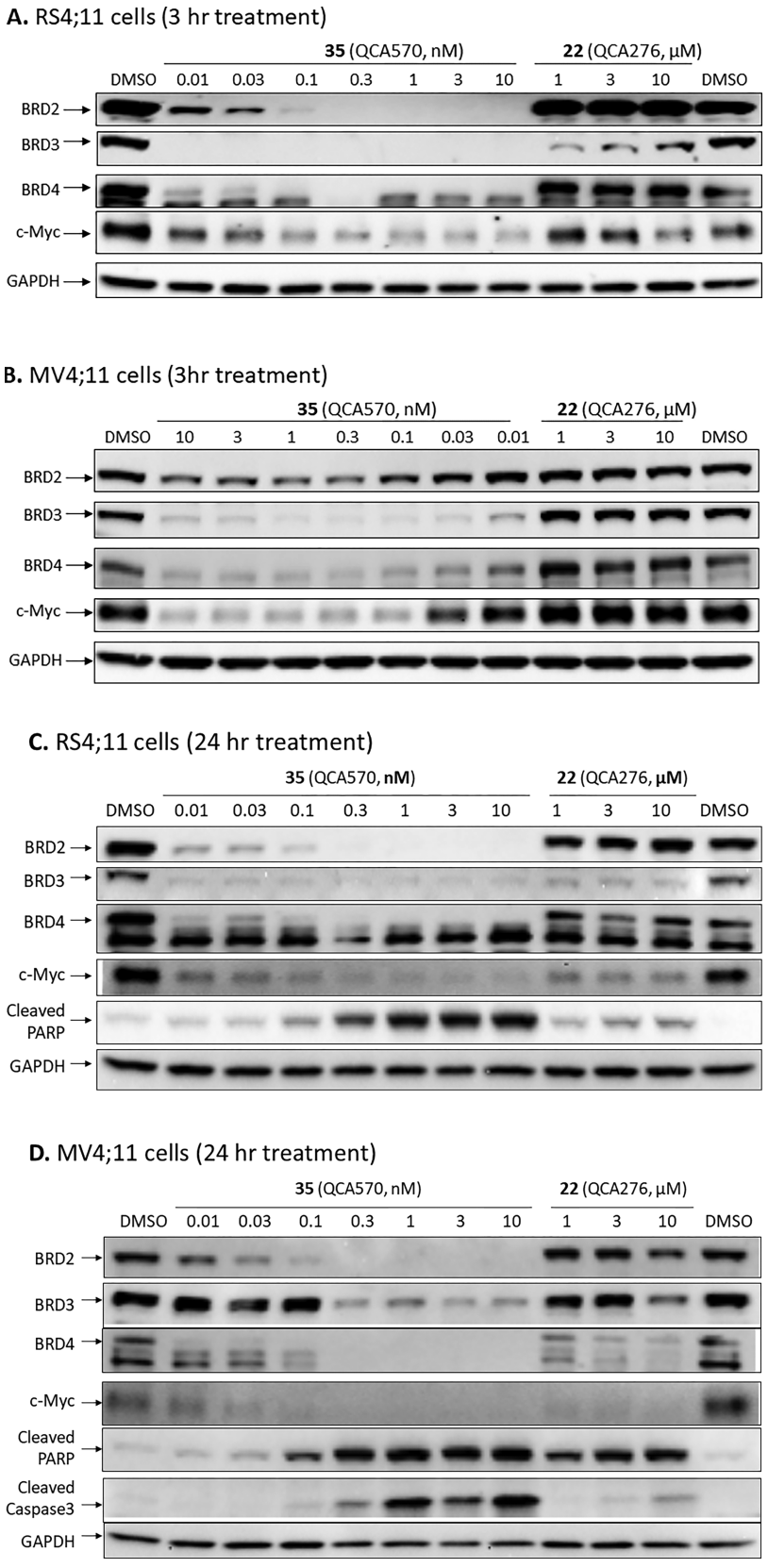

Figure 4. Western blotting analysis of BRD2, BRD3, and BRD4 proteins, c-Myc, and cleaved PARP in RS4;11 (A,C) and MV4;11 (B,D) leukemia cells treated with BET degrader **35** (QCA570) and the corresponding BET inhibitor **22** (QCA276). RS4;11 or MV4;11 cells were treated for 3 h (A,B) or 24 h (C,D) at indicated concentrations with **35** or **22**. Proteins were probed using specific antibodies.

We evaluated a number of previously published BET degraders such as dBET1,[43] ARV-825,[37] ARV-771,[47] and ZBC260[44] for their cell growth inhibitory activity in these three leukemia cell lines (Table 3). Consistent with the previous

DOI: 10.1021/acs.jmedchem.8b00506
J. Med. Chem. XXXX, XXX, XXX−XXX

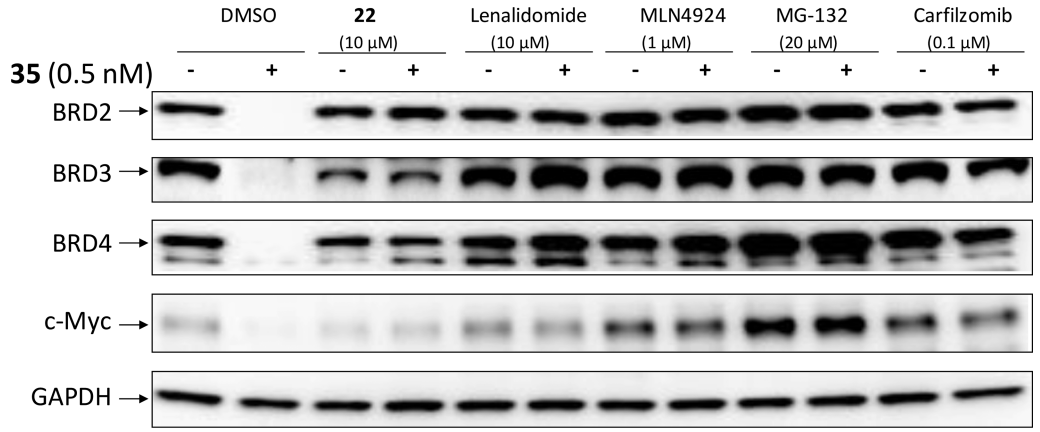

Figure 5. Evaluation of the mechanism of action of BET degradation induced by **35** (QCA570). RS4;11 cells were pretreated for 2 h with DMSO, BET inhibitor **22** (10 μM), cereblon ligand lenalidomide (10 μM), E1 neddylation inhibitor MLN4924 (1 μM), or proteasome inhibitors MG-132 (20 μM) and Carfilzomib (0.1 μM). Cells were then treated for 3 h with BET degrader **35** (QCA570) at 0.5 nM, a concentration that induces complete degradation of all BET-BRD proteins and downregulation of c-Myc.

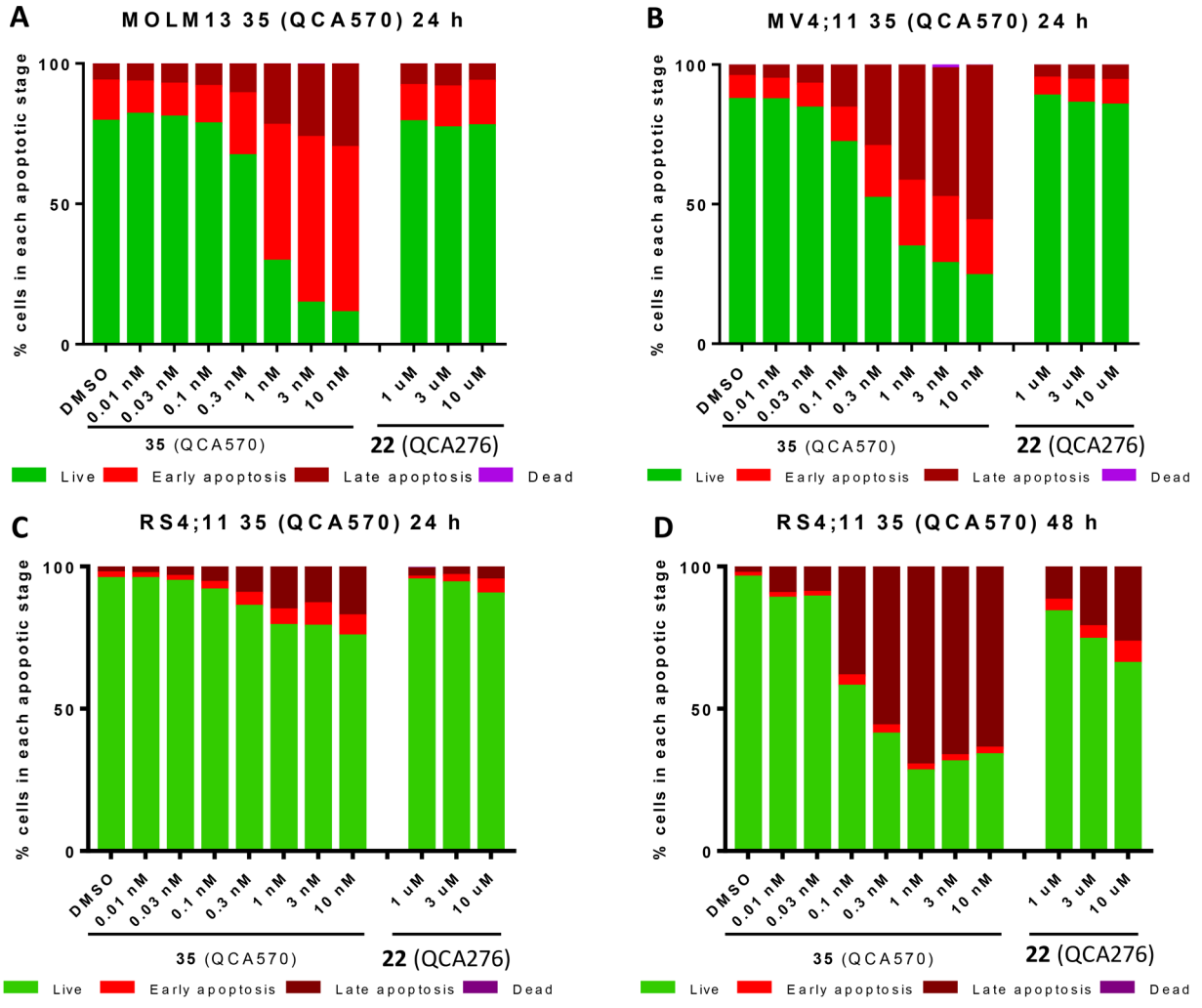

Figure 6. Flow cytometry analysis of apoptosis induction by **35** (QCA570) in MOLM13 (A), MV4;11 (B), and RS4;11 (C,D) leukemia cells. Cells were treated with the BET degrader **35** (QCA570) or the corresponding BET inhibitor (**22**) at the indicated concentrations for 24 h (A–C) or 48 h (D). Apoptosis was assessed by flow cytometry using Annexin V and propidium iodine (PI) double staining.

studies, these BET degraders all potently inhibit cell growth in these leukemia cell lines (Table 3). In direct comparison, **35** is >1000-times more potent than dBET1 and at least >10-times more potent than ARV-825 and ARV-771 in each of these three cell lines. Although ZBC260 and **35** have similar potencies in the RS4;11 cell line, **35** is >10-times more potent than ZBC260 in the MV4;11 and MOLM-13 cell lines. Based on these data, **35** is the most potent BET degrader reported to date.

DOI: 10.1021/acs.jmedchem.8b00506
J. Med. Chem. XXXX, XXX, XXX−XXX

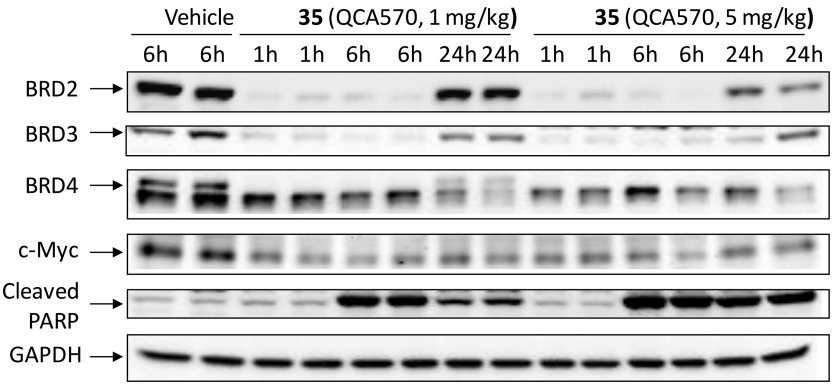

Figure 7. Pharmacodynamic analysis of compound **35** in RS4;11 xenograft tumors. SCID mice bearing RS4;11 tumors were treated with a single intravenous dose of compound **35** at 1 or 5 mg/kg. At the indicated time points (1, 6, and 24 h), mice were sacrificed and tumors were harvested. Tumors were lysed for Western blotting analysis of BRD2, BRD3, BRD4, c-Myc, and cleaved PARP. GAPDH was used as the loading control. Two mice were used for each time-point with each mouse bearing one tumor.

Table 4. Tissue Distribution of Compound 35 (QCA570) in Mice Bearing RS4;11 Xenograft Tumors[a]

	concentrations of QCA570 in plasma (ng/mL) and tissues (ng/g)								
(IV, 5 mg/kg)	mouse 1 (1 h)	mouse 2 (1 h)	mouse 3 (3 h)	mouse 4 (3 h)	mouse 5 (6 h)	mouse 6 (6 h)	mean (1 h)	mean (3 h)	mean (6 h)
plasma	1575	2360	47	263	BLQ	BLQ	1968	155	BLQ
Tumor	642	405	177	199	87.9	68.7	524	188	78
Liver	1227	1720	57	209	BLQ	BLQ	1473	133	BLQ
Heart	373	288	17	22	BLQ	BLQ	331	19	BLQ
Kidney	649	675	40	49	BLQ	BLQ	662	44	BLQ
Lung	1041	696	35	89	BLQ	BLQ	868	62	BLQ
Intestine	1283	1009	50	92	BLQ	BLQ	1146	71	BLQ

[a]Each mouse had one tumor and was dosed with a single, intravenous dose of compound **35**. Mice were sacrificed at 1, 3, and 6 h time-points, and different tissues were collected for analysis of drug concentration by LC/MS/MS. BLQ, below the limit of quantification.

We next investigated the ability of **35** to induce degradation of BET proteins in the MV4;11 and RS4;11 cell lines and its suppression of c-Myc protein expression (Figure 4). At concentrations as low as 10 pM, **35** is very effective in reducing the levels of BRD3 and BRD4 proteins and that of the BRD2 protein at 30−100 pM in both leukemia cell lines with a 3 h treatment (Figure 4A,B). Consistently, compound **35**, at concentrations as low as 10 pM in the RS4;11 cell line and 30 pM in the MV4;11 cell line, is very effective in reducing the levels of c-Myc protein. The corresponding BET inhibitor (**22**) fails to reduce the levels of BRD2, BRD3, and BRD4 proteins in the MV4;11 cell line and the levels of BRD2 and BRD4 proteins in the RS4;11 cell line. Interestingly, the level of BRD3 protein was reduced by **22** in the RS4;11 cell line but not in the MV4;11 cell line.

We investigated the mechanism of action for the degradation of BET proteins induced by **35**. Compound **35** at a concentration of 0.5 nM induced complete degradation of BRD2, BRD3, and BRD4 proteins in the RS4;11 cell line with a 3 h treatment time (Figure 5). Degradation of BRD2, BRD3, and BRD4 proteins by **35** is completely blocked by pretreatment with lenalidomide, a ligand for cereblon; MLN4924, an E1 neddylation inhibitor; or MG-132 and carfizomib, two proteasome inhibitors. Therefore, these data clearly demonstrate that **35** induces degradation of BRD2, BRD3, and BRD4 proteins through cereblon-, neddylation-, and proteasome-dependent mechanisms, consistent with its PROTAC design.

A previous study showed that an analogue of lenalidomide can elicit strong antitumor activity by inducing degradation of GSPT1.[55] To further investigate the mechanism of action for **35**, we examined the effect of **35** on GSPT1 protein in both the MV4;11 and RS4;11 cells. Our Western blotting data showed that, while **35** is highly potent and effective in inducing degradation of BRD2, BRD3, and BRD4 proteins, it has no effect on GSPT1 protein (SI, Figure S2).

We used flow cytometry to investigate the ability of **35** to induce apoptosis in the MV4;11, MOLM-13, and RS4;11 cell lines and found that **35** is highly potent and effective in inducing apoptosis in a dose-dependent manner (Figure 6). In both the MOLM-13 and MV4;11 cell lines, it induces >60% of the cells to undergo apoptosis at concentrations as low as 1 nM upon a 24 h treatment (Figure 6A,B). It is interesting that **35** has slower kinetics of apoptosis induction in the RS4;11 cell line than that in the MOLM-13 and MV4;11 cell lines. With 24 h treatment time, **35** has a minimal effect at 0.1 nM and induces only 15−30% of the RS4;11 cells to undergo apoptosis at 0.3−10 nM (Figure 6C). However, with a 48 h treatment time, **35** is highly effective in inducing apoptosis at concentrations as low as 0.1 nM; **35** induces >40% of the RS4;11 cells to undergo apoptosis at 0.1 nM (Figure 6D). In direct comparison, the corresponding BET inhibitor **22**, at concentrations of 1−10 μM, has only a minimal to modest effect in induction of apoptosis in these three cell lines.

Consistent with the strong effect on apoptosis induction by **35** determined in the flow cytometry assay, our Western blotting analysis showed that it induces robust cleavage of PARP at concentrations as low as 0.1−0.3 nM in the MV4;11 and RS4;11 cell lines after 24 h treatment (Figure 4C,D). Also in agreement with our flow cytometry data, **35** induces caspase 3 activation at concentrations as low as 0.3 nM in the MV4;11 cell line. Caspase

DOI: 10.1021/acs.jmedchem.8b00506
J. Med. Chem. XXXX, XXX, XXX−XXX

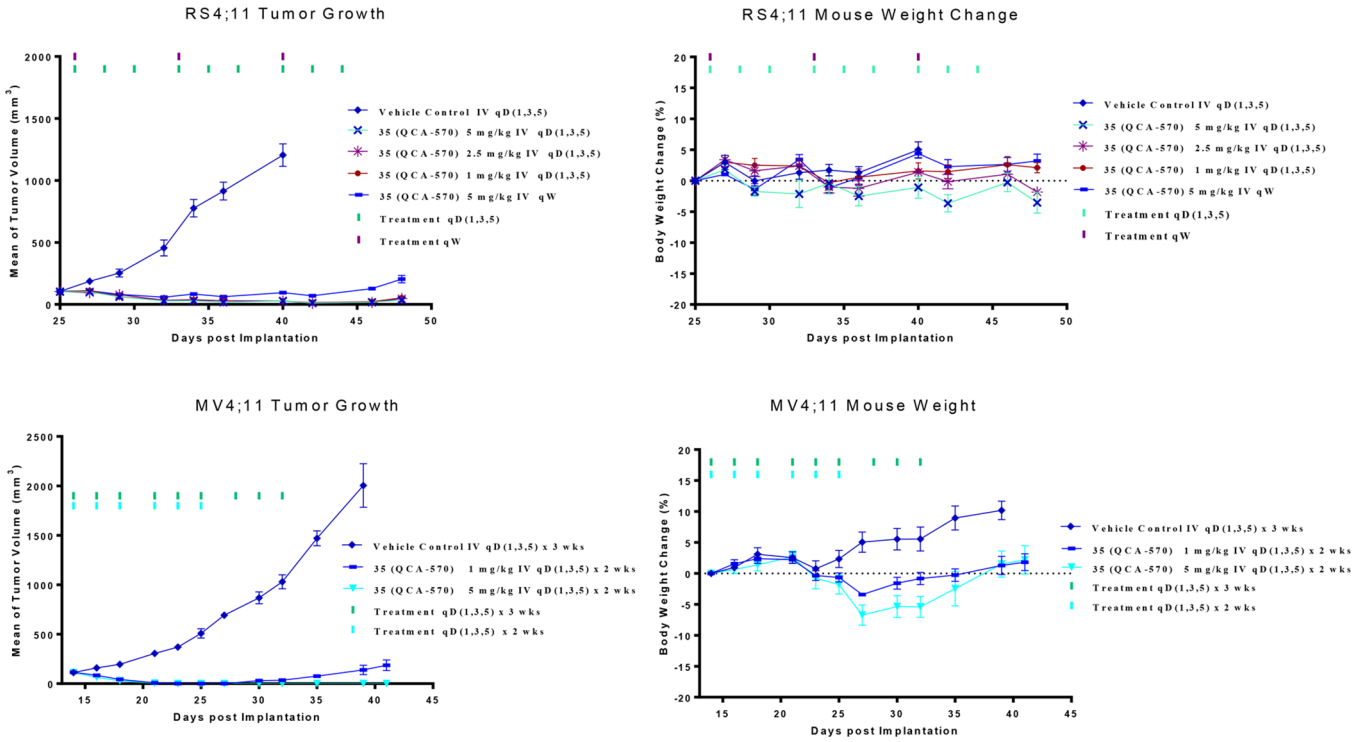

Figure 8. *In vivo* anticancer efficacy of BET degrader (**35**) in the RS4;11 and MV4;11 xenograft models in mice. (A,B) Mice bearing RS4;11 tumors were treated with BET degrader **35** at different dose-schedules: (A) tumor growth and (B) animal weights. (C,D) Mice bearing MV4;11 tumors were treated with BET degrader (**35**) at 1 or 5 mg/kg three times a week for 2 weeks by intravenous dosing: (C) tumor growth and (D) animal weights.

Scheme 1. Synthetic Route to Compound 22 (QCA276)[a]

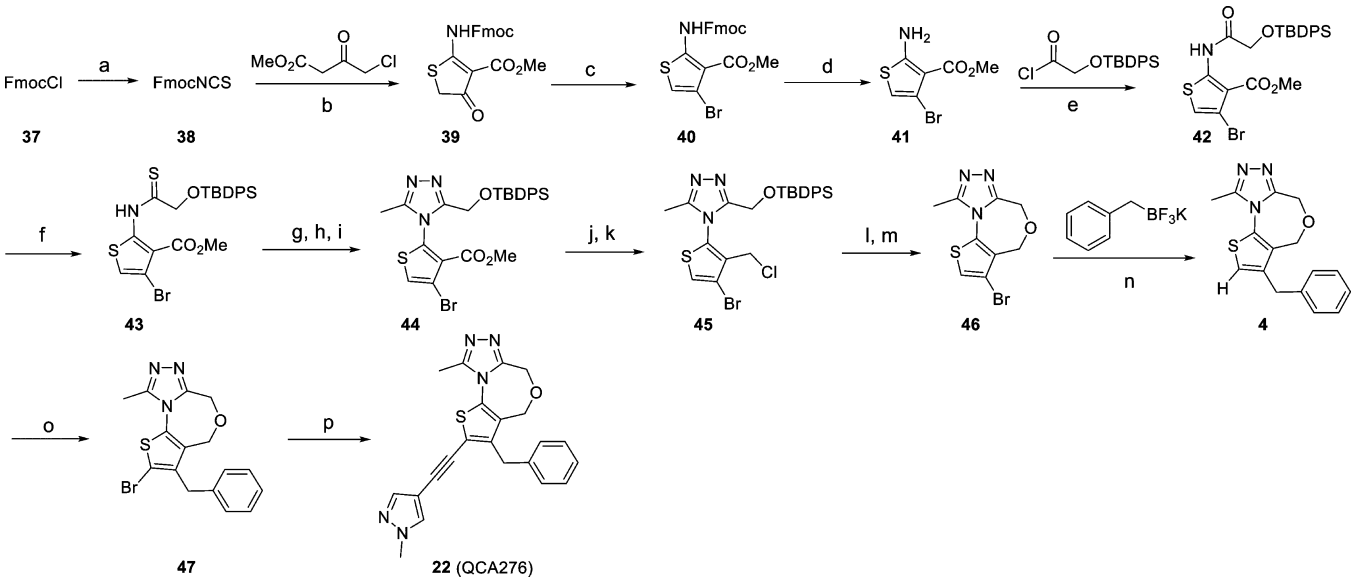

[a]Reaction Conditions: (a) KNCS, EtOAc, 0 °C−r.t., 92%; (b) NaH, THF, 0 °C, 62%; (c) $POBr_3$; (d) morpholine, 52% yield over two steps; (e) DIPEA, DCM, 99%; (f) Lawesson's reagent, dioxane, 57%; (g) $NH_2NH_2{\cdot}H_2O$; (h) $MeC(OEt)_3$; (i) AcOH, 58% yield over three steps; (j) $LiBH_4$; (k) $SOCl_2$, 77% yield over two steps; (l) TBAF; (m) NaO*t*-Bu, 66% yield over two steps; (n) Pd(allyl)Cl_2, ^{s}SPhos, Na_2CO_3, H_2O, toluene, 77%; (o) NBS, HOAc, 84%; (p) $PdCl_2(PPh_3)_2$, CuI, THF, Et_3N, 92%.

3 cleavage was not detected in the RS4;11 cell line with the 24 h treatment, consistent with the slow kinetics in apoptosis induction by **35** in this cell line that was revealed by flow cytometry analysis.

Next, we investigated the effect of **35** *in vivo* in a pharmacodynamics experiment using RS4;11 xenograft tumors in mice (Figure 7). SCID mice bearing the RS4;11 tumors were administered a single, intravenous dose of **35** at 1 or 5 mg/kg, and tumor tissues were harvested for analysis at 1, 6, and 24 h after drug treatment. Western blotting analysis showed that **35** dramatically reduces the levels of BRD2, BRD3, and BRD4 proteins at the 1 and 6 h time-points at both 1 and 5 mg/kg doses and is more effective in reducing the BRD4 protein level at the 24 h time-point with 5 mg/kg than with 1 mg/kg. Consistent

DOI: 10.1021/acs.jmedchem.8b00506
J. Med. Chem. XXXX, XXX, XXX−XXX

Scheme 2. Synthesis of BET Degrader 35 (QCA570)[a]

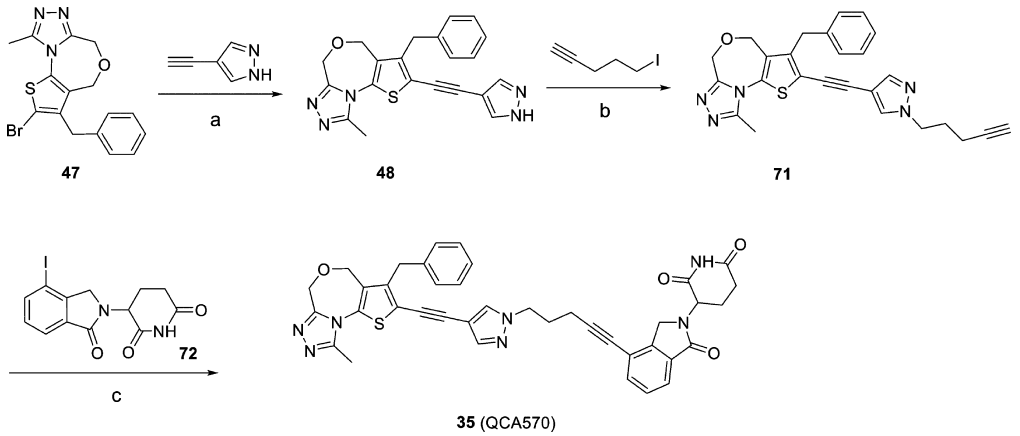

[a]Reaction conditions: (a) $PdCl_2(PPh_3)_2$, CuI, THF, Et_3N, 70%; (b) K_2CO_3, DMF, 80%; (c) $PdCl_2(PPh_3)_2$, CuI, THF, Et_3N, 54%.

with the profound reduction of BRD2, BRD3, and BRD4 proteins in the RS4;11 tumor tissue, **35** with both 1 and 5 mg/kg treatments reduces c-Myc protein levels dramatically at all the time points examined. Compound **35** is also very effective in inducing cleavage of PARP at the 6 and 24 h time-points, indicating strong apoptosis induction in the tumor tissue.

We performed tissue distribution analysis of compound **35** in mice bearing RS4;11 xenograft tumors, with the data summarized in Table 4. Our data showed that compound **35** is extensively distributed into all the tissues collected and analyzed. Compound **35** has good exposure in all tissues at 1 h time-point. The concentration of **35** is rapidly deceased at 3 h time-point and becomes undetectable at 6 h time-point, with the exception in the xenograft tumor tissue. Since **35** is capable of inducing rapid degradation of BET proteins in cells even at concentration of <1 nM, our tissue distribution data suggest that a single dose of **35** at 5 mg/kg can achieve sufficient exposure to induce degradation of BET proteins in all tissues.

We tested **35** for its antitumor efficacy in the RS4;11 and MV4;11 xenograft models, and the data are summarized in Figure 8. In the RS4;11 xenograft model, **35** achieved complete and long-lasting tumor regression with doses of 1, 2.5, and 5 mg/kg, three times per week for 3 weeks (Figure 8A). Compound **35** at 5 mg/kg weekly was also very effective, achieving complete tumor growth inhibition but not tumor regression (Figure 8A). Compound **35** induced minimal animal weight loss (Figure 8B), and there were no other signs of toxicity in all the treatment groups.

In the MV4;11 xenograft model, **35** achieved complete tumor regression at 1 mg/kg, three times per week for 2 weeks (Figure 8C). At 5 mg/kg, three times per week for 2 weeks, compound **35** achieves complete and long-lasting tumor regression (Figure 8C). It caused a maximum weight loss of less than 10% in the MV4;11 model (Figure 8D). Taken together, these studies demonstrate that compound **35** is highly efficacious at well-tolerated, dose schedules.

Chemistry. The synthesis of the BET inhibitor **22** is shown in Scheme 1. Briefly, FmocCl (**37**) was converted to FmocNCS (**38**). Cyclization with methyl 4-chloro-3-oxobutanoate followed by bromination with phosphorus(V) oxybromide resulted in Fmoc-protected methyl 2-amino-4-bromothiophene-3-carboxylate (**40**), and removal of the protecting groups afforded **41**. The amino group of **41** was reacted with 2-(OTBDPS) acetic chloride to give the amide (**42**), which was transformed into the sulfamide (**43**) using Lawesson's reagent. A subsequent three-step cyclization generated the triazole (**44**), whose methyl carboxylate group was reduced, then chlorinated to generate a methylene chloride group, which linked with the unprotected hydroxyl group to form the seven-membered oxygen-containing ring in **46**. A benzyl group was introduced into the thiophene through a palladium-catalyzed Suzuki coupling reaction giving the benzyl-substituted thiophene (**4**). Bromination of **4** gave compound **47**, and finally, Sonogashira coupling of **47** with 4-ethynyl-1-methyl-1*H*-pyrazole gave compound **22** (QCA276).

The synthetic route to the BET degrader (**35**) is shown in Scheme 2. Introduction of 4-ethynyl-1*H*-pyrazole to compound **47** produced compound **48**, alkylation of which with 5-iodopent-1-yne generated **71**. Sonogashira coupling of **71** with 3-(4-iodo-1-oxoisoindolin-2-yl)piperidine-2,6-dione gave the final compound **35**.

CONCLUSIONS

In this study, we present our design, synthesis, and evaluation of novel PROTAC degraders of BET proteins using a new class of BET inhibitors we have designed and known cereblon ligands. Our study has led to the discovery of a set of extremely potent and highly efficacious BET degraders, exemplified by **35** (QCA570). QCA570 is capable of effectively inducing degradation of BRD2, BRD3, and BRD4 proteins at low picomolar concentrations in human leukemia cell lines and has picomolar IC_{50} values in inhibition of cell growth in the MV4;11, RS4;11, and MOLM-13 human leukemia cell lines. Significantly, QCA570 achieves complete and long-lasting tumor regression in both the MV4;11 and RS4;11 acute leukemia xenograft models in mice at well-tolerated dose schedules. Our data demonstrate that QCA570 is the most potent and efficacious BET degrader reported to date and warrants extensive further investigation as a potential therapy for the treatment of acute leukemia and other types of human cancer.

EXPERIMENTAL SECTION

Chemistry. General Methods. Unless otherwise noted, all purchased reagents were used as received without further purification. ^1H NMR and ^{13}C NMR spectra were recorded on Bruker Advance 400 and 300 MHz spectrometers. ^1H NMR spectra were reported in parts per million (ppm) referenced to 7.26 ppm of $CDCl_3$ or referenced to the center line of a septet at 2.50 ppm of DMSO-d_6 or 3.31 ppm of

DOI: 10.1021/acs.jmedchem.8b00506
J. Med. Chem. XXXX, XXX, XXX−XXX

CD_3OD. All ^{13}C NMR spectra were reported in ppm and obtained with ^1H decoupling. In the reported spectral data, the format (δ) chemical shift (multiplicity, J values in Hz, integration) was used with the following abbreviations: s = singlet, d = doublet, t = triplet, q = quartet, m = multiplet. MS analyses were carried out on a Waters UPLC-Mass instrument. The final compounds were all purified by C18 reverse phase preparative HPLC column with solvent A (0.1% TFA in H_2O) and solvent B (0.1% TFA in CH_3CN) as eluents. The purities of all the final compounds were confirmed to be >95% by UPLC−MS or UPLC.

*General Procedure for Synthesis of Compound **3** and Compounds **5**−**7**.* NBS (716 mg, 4.02 mmol) was added to a solution of compound **4** (0.8 g, 2.68 mmol) in HOAc (25 mL). The reaction mixture was stirred at room temperature for 6 h. If compound **4** was not consumed completely, more NBS was added. All volatiles were removed, and the residue was chromatographed on silica gel (DCM and MeOH) to afford compound **47** (950 mg, 84%).

A Shlenk tube was charged with compound **47** (10 mg), the corresponding boronic acid pinacol ester (2.0 equiv), $Pd_2(dba)_3$ (2.7 mg), PCy_3 (1.7 mg), dioxane (1 mL), and Na_2CO_3 solution (2 M, 0.5 mL) under N_2. The tube was then sealed and heated at 100 °C in an oil bath for 4 h. The reaction mixture was extracted with EtOAc, and the organic layer was washed with brine, dried, and concentrated. The residue was purified through HPLC to afford compound **3** and compounds **5**−**7**.

*3-Benzyl-2,9-dimethyl-4H,6H-thieno[2,3-e][1,2,4]triazolo[3,4-c]-[1,4]oxazepine (**3**).* ^1H NMR (400 MHz, $CDCl_3$) δ 7.51−7.21 (m, 4H), 7.07 (d, J = 7.2 Hz, 2H), 4.82 (s, 2H), 4.72 (s, 2H), 3.88 (s, 2H), 2.96 (s, 3H), 2.52 (s, 3H). ESI-MS $[M + H]^+$: 312.20. UPLC: 4.2 min.

*3-Benzyl-9-methyl-4H,6H-thieno[2,3-e][1,2,4]triazolo[3,4-c][1,4]-oxazepine (**4**).* Compound **37** (52 g, 200 mmol) in EtOAc (200 mL) was added dropwise to a suspension of anhydrous KSCN (21.4 g, 2200 mmol) in EtOAc (200 mL) at 0 °C. The reaction mixture was allowed to warm to r.t. and stirred overnight. The reaction mixture was filtered, and the filtrate was evaporated under vacuum. NMR analysis of the crude showed a small amount of the solvent EtOAc. The crude product was treated with DCM (100 mL) and hexanes (100 mL), and the resulting solution was evaporated under vacuum to facilitate removal of the small amount of EtOAc. The yield of crude compound **38** was 52 g, 92%.

A solution of methyl 4-chloro-3-oxobutanoate (30.1 g, 200 mmol, 1.1 equiv) in THF (50 mL) was added dropwise to a suspension of NaH (60% in mineral oil, 8.8 g, 220 mmol, 1.2 equiv) in THF (200 mL) at 0 °C. After the addition was complete, the reaction mixture was allowed to warm to r.t. and stirred for 20 min. Then the reaction mixture was cooled to 0 °C and a solution of crude FmocNCS (52 g, 184 mmol) in THF (50 mL) was added dropwise. After the addition was complete, the reaction mixture was quenched at 0 °C by the addition of 50 mL of saturated NH_4Cl solution and 50 mL of H_2O. Then the majority of the solvent was evaporated under vacuum when, at this time point, a precipitate started to form. Then 150 mL of H_2O and 150 mL of EtOAc were added, and the mixture was stirred at room temperature until it became a suspension. The crude mixture was filtered, and occasional stirring of the filter cake was used to speed up the filtration process. The filter cake was further rinsed with H_2O (100 mL) and EtOAc (100 mL). Again the filter cake was stirred occasionally during the washing process to facilitate filtration. The filter cake (56.3 g) was transferred to a flask. This crude product was further dried under high vacuum overnight to remove H_2O and the organic solvent. After drying, the crude compound (**39**) weighed 44.9 g (62% yield) as a light yellow solid. ^1H NMR (400 MHz, $CDCl_3$) δ 11.90 (s, 1H), 7.81 (d, J = 6.5 Hz, 2H), 7.62 (d, J = 7.4 Hz, 2H), 7.48−7.38 (m, 2H), 7.37 (d, J = 6.7 Hz, 2H), 4.59 (d, J = 6.9 Hz, 2H), 4.37−4.29 (m, 1H), 3.94 (s, 2H), 3.66 (s, 2H).

$POBr_3$ (39 g, 137 mmol, 1.2 equiv) was added to a suspension of compound **39**, methyl 2-((((9*H*-fluorene-9-yl)methoxy)carbonyl)-amino)-4-oxo-4,5-dihydrothiophene-3-carboxylate (44.9 g, 114 mmol) in dioxane (250 mL), and the reaction mixture was heated to 100 °C. The reaction was monitored by TLC, which showed all the starting material to have been consumed in less than 1 h. The reaction mixture was cooled and poured into the mixture of ice−water. The reaction mixture was extracted with EtOAc (3 × 300 mL). The combined organic layers were washed with brine twice, dried over Na_2SO_4, and concentrated. The crude product compound (**40**) was used directly in the next step.

The residue was dissolved in DCM (75 mL), and the reaction mixture was cooled to 0 °C. Morpholine (52 mL, 5 equiv) was added slowly, and the reaction mixture was allowed to warm to room temperature then stirred overnight. The reaction mixture was filtered and rinsed with a small amount of Et_2O. The filtrate was evaporated under vacuum, and the residue was chromatographed on silica gel (pure DCM) to afford 2-amino-4-bromothiophene-3-carboxylate (**41**), as an off-white solid (14 g, 52% over two steps).

2-((*tert*-Butyldiphenylsilyl)oxy)acetic acid (6 g, 19 mmol) was dissolved in DCM (60 mL), and the solution was cooled to 0 °C under N_2. Oxalyl chloride (1.3 eq, 25 mmol, 2.1 mL) was added followed by the addition of DMF (0.1 mL). The mixture was allowed to warm to r.t. and stirred for a further 1 h. All the volatiles were removed under vacuum, and the residue was dissolved in DCM (10 mL). This solution was added to a solution of compound **41** (2.36 g, 10 mmol) in DCM (60 mL) and DIPEA (5.2 mL, 30 mmol) at 0 °C under N_2. The reaction mixture was allowed to warm to r.t. and stirred for 1 h prior to being quenched with saturated $NaHCO_3$ and extracted with DCM (3 × 50 mL). The combined organic layer was washed with H_2O and then dried with Na_2SO_4, filtered, and concentrated. The oil was chromatographed on silica gel (1:16 to 1:8 EtOAc/hexanes) to give compound **42** as an oil (5.3 g, 99%).

Lawesson's reagent (2.4 g, 6 mmol, 0.6 equiv) was added to a solution of compound **42** (5.5 g, 10 mmol) in dioxane (40 mL), and the reaction mixture was heated at reflux. The reaction was monitored by TLC, and all the starting material was consumed in 4−6 h. The reaction mixture was cooled and diluted with H_2O and EtOAc. After extraction, the organic layers were combined and washed with brine twice. The organic layer was dried and removed under vacuum. The residue was chromatographed on silica gel (1:16 to 1:8 EtOAc/hexanes) to give compound **43** as an oil (3.2 g, 57%).

Hydrazine monohydrate (0.55 mL, 11.4 mmol, 2 equiv) was added at r.t. to a solution of compound **43** (3.2 g, 5.7 mmol) in THF (20 mL). The reaction mixture was stirred for 1 h and then concentrated in vacuum. The residue was taken up in DCM and washed with H_2O and brine. The organic layer was separated, dried, and concentrated. The residue was taken up in EtOH (10 mL) and THF (2 mL), and triethyl orthoacetate (3.1 mL, 3 equiv) was added. The reaction mixture was heated at reflux for 1 h. All volatiles were removed under vacuum, and the residue was treated with AcOH (20 mL). The reaction mixture was heated at reflux for 1 h prior to the removal of the solvent under vacuum. The residue was treated with EtOAc and washed with 1 M NaOH, saturated $NaHCO_3$, and brine. The organic layer was dried and concentrated. The residue was chromatographed on silica gel (1:2 EtOAc/hexanes followed by EtOAc, then DCM/MeOH 15:1) to give compound **44** (1.9 g, 58%).

A solution of $LiBH_4$ (2 M in THF, 3.3 mL, 6.6 mmol, 2 equiv). MeOH (2 mL) was added at 0 °C to a solution of compound **44** (1.9 g, 3.3 mmol) in THF (20 mL), and the reaction mixture was allowed to warm to r.t., then stirred for 12 h. All volatiles were removed, and the residue was taken up in EtOAc. The organic layer was washed with H_2O and brine prior to being dried and concentrated. The residue was dissolved in DCM (20 mL) and cooled to 0 °C. Thionyl chloride (0.72 mL, 9.9 mmol, 3 equiv) was added, and the reaction mixture was allowed to warm to r.t. After 1 h, all the volatiles were removed, and the residue was taken up in EtOAc and washed with 1 M Na_2CO_3 and brine, dried, and concentrated to give crude compound **45** (1.75 g).

A solution of TBAF (3.1 mL, 3.1 mmol, 1 M in THF) was added to a solution of compound **45** (1.75 g, 3.1 mmol) in THF (10 mL). The solution was stirred for 1 h prior to being added to a heated solution of *t*-BuONa (595 mg, 6.2 mmol, 2 equiv) in *t*-BuOH (40 mL) at 80 °C. The reaction mixture was stirred for 5 min and then cooled. All the solvent was removed under vacuum, and the residue was taken up in EtOAc and H_2O. The organic layer was washed with brine, dried, and concentrated. The residue was purified by HPLC to afford the TFA salt of the compound **46** (667 mg, 51% over four steps).

DOI: 10.1021/acs.jmedchem.8b00506
J. Med. Chem. XXXX, XXX, XXX−XXX

A solution of Na_2CO_3 (2 M in H_2O, 10 mL) and H_2O (10 mL) was added to a solution of compound **46** (1.0 g, 3.5 mmol), Pd(ally)Cl_2 (10% mmol), sodium 2′-dicyclohexylphosphino-2,6-dimethoxy-1,1′-biphenyl-3-sulfonate hydrate (sSPhos) (20% mmol), and potassium benzyltrifluoroborate (1.39 g, 7.0 mmol) in toluene (25 mL). The reaction mixture was stirred at room temperature for 30 min and then heated to 110 °C and stirred for 3−4 h. All volatiles were removed, and the residue was dissolved in EtOAc. The organic layer was washed with water and brine prior to being dried and concentrated. The residue was chromatographed on silica gel (DCM and MeOH) to afford compound **4** (800 mg, 77%). ^{1}H NMR (400 MHz, $CDCl_3$) δ 7.40−7.30 (m, 3H), 7.20 (d, J = 7.2 Hz, 2H), 6.82 (s, 1H), 4.79 (s, 2H), 4.73 (s, 2H), 3.88 (s, 2H), 2.75 (s, 3H). Retention time: 4.37 min; ESI-MS $[M + H]^+$: 298.10. UPLC: 3.4 min.

*3-Benzyl-2-isopropyl-9-methyl-4H,6H-thieno[2,3-e][1,2,4]-triazolo[3,4-c][1,4]oxazepine (**5**).* ^{1}H NMR (400 MHz, MeOD) δ 7.30 (d, J = 7.4 Hz, 2H), 7.21 (t, J = 7.4 Hz, 1H), 7.13 (d, J = 7.1 Hz, 2H), 4.72 (s, 2H), 4.66 (s, 2H), 4.00 (s, 2H), 3.50−3.43 (m, 1H), 2.81 (s, 3H), 1.34 (d, J = 6.8 Hz, 6H). ESI-MS: 340.02. UPLC: 5.9 min.

*3-Benzyl-9-methyl-2-(tetrahydro-2H-pyran-4-yl)-4H,6H-thieno-[2,3-e][1,2,4]triazolo[3,4-c][1,4]oxazepine (**6**).* ^{1}H NMR (400 MHz, MeOD) δ 7.30 (t, J = 7.4 Hz, 2H), 7.22 (t, J = 7.3 Hz, 1H), 7.13 (d, J = 7.1 Hz, 2H), 4.71 (s, 2H), 4.66 (s, 2H), 4.03 (s, 2H), 4.01−3.95 (m, 1H), 3.65−3.42 (m, 3H), 3.40−3.35 (m, 1H), 2.78 (s, 3H), 1.97−1.69 (m, 4H). ESI-MS: 382.09. UPLC: 4.9 min.

*3-Benzyl-2-(tert-butyl)-9-methyl-4H,6H-thieno[2,3-e][1,2,4]-triazolo[3,4-c][1,4]oxazepine (**7**).* ^{1}H NMR (400 MHz, MeOD) δ 7.30 (t, J = 7.6 Hz, 3H), 7.22 (d, J = 6.8 Hz, 1H), 7.18 (d, J = 7.7 Hz, 2H), 4.73 (s, 2H), 4.68 (s, 2H), 4.09 (s, 2H), 2.79 (d, J = 0.6 Hz, 3H), 2.22−2.10 (m, 1H), 1.11 (q, J = 5.0 Hz, 2H), 0.79 (q, J = 4.9 Hz, 2H). ESI-MS: M + H 338.18.

*General Procedure for Synthesis of Compounds **8** and **10**−**25**.* The corresponding alkyne (2.0 equiv), Pd$(PPh_3)_2Cl_2$ (4.2 mg), CuI (2.3 mg), THF (1 mL), and Et_3N (1 mL) were added under N_2 to a flask charged with **47** (20 mg, 0.05 mmol). The reaction mixture was stirred at 60 °C for 18 h. The reaction mixture was extracted with EtOAc, and the organic layer was washed with brine, dried, and concentrated. The residue was purified through HPLC to afford compounds **8** and **10**−**25**.

*3-Benzyl-2-ethynyl-9-methyl-4H,6H-thieno[2,3-e][1,2,4]triazolo-[3,4-c][1,4]oxazepine (**8**).* Obtained by coupling of **47** with TMS-acetylene followed by treatment with TBAF to remove the TMS group. ^{1}H NMR (400 MHz, MeOD) δ 7.37−7.16 (m, 5H), 4.72 (s, 2H), 4.69 (s, 2H), 4.22 (s, 1H), 4.10 (s, 2H), 2.76 (s, 3H). ESI-MS: 322.20. UPLC: 4.9 min.

*3-Benzyl-9-methyl-4H,6H-thieno[2,3-e][1,2,4]triazolo[3,4-c][1,4]-oxazepine-2-carbonitrile (**9**).* A flask was charged with compound **47** (20 mg, 0.05 mmol), $K_3Fe(CN)_6$ (7 mg), CuI (2 mg), and 1-methyl-1*H*-imidazole (0.5 mL) under N_2. The reaction mixture was stirred at 140 °C for 18 h. The reaction mixture was extracted with EtOAc, and the organic layer was washed with brine, dried, and concentrated. The residue was purified through HPLC to afford compound **9** (45% yield). ^{1}H NMR (400 MHz, MeOD) δ 7.35 (t, J = 7.3 Hz, 2H), 7.28 (d, J = 7.3 Hz, 1H), 7.27−7.20 (m, 2H), 4.77 (s, 2H), 4.76 (s, 2H), 4.18 (s, 2H), 2.79 (s, 3H). ESI-MS: 323.20.

*4-(3-Benzyl-9-methyl-4H,6H-thieno[2,3-e][1,2,4]triazolo[3,4-c]-[1,4]oxazepin-2-yl)but-3-yn-1-ol (**10**).* ^{1}H NMR (400 MHz, MeOD) δ 7.29 (t, J = 7.5 Hz, 2H), 7.25−7.15 (m, 3H), 4.72 (s, 2H), 4.69 (s, 2H), 4.06 (s, 2H), 3.75 (t, J = 6.5 Hz, 2H), 2.75−2.70 (m, 5H). ESI-MS: 366.11.

*3-(3-Benzyl-9-methyl-4H,6H-thieno[2,3-e][1,2,4]triazolo[3,4-c]-[1,4]oxazepin-2-yl)-N,N-dimethylprop-2-yn-1-amine (**11**).* ^{1}H NMR (400 MHz, MeOD) δ = 7.29 (dd, J = 7.0 Hz, J = 7.6 Hz, 2H), 7.21 (d, J = 7.0 Hz, 1H), 7.17 (d, J = 7.6 Hz, 2H), 4.73 (s, 2H), 4.70 (s, 2H), 4.41 (s, 2H), 4.11 (s, 2H), 2.94 (s, 6H), 2.77 (s, 3H). ^{13}C NMR (100 MHz, MeOD) 146.4, 138.9, 132.6, 132.3, 129.9, 129.2, 127.9, 116.1, 87.0, 81.9, 69.0, 62.8, 48.4, 42.8, 34.6, 12.5. ESI-MS: 379.33. UPLC: 1.6 min.

*3-Benzyl-9-methyl-2-(3-methylbut-1-yn-1-yl)-4H,6H-thieno[2,3-e][1,2,4]triazolo[3,4-c][1,4]oxazepine (**12**).* ^{1}H NMR (400 MHz, MeOD) δ = 7.31−7.22 (m, 2H), 7.24−7.15 (m, 3H), 4.70 (s, 2H), 4.69 (s, 2H), 4.00 (s, 2H), 2.90−2.82 (m, 1H), 2.75 (s, 3H), 1.26 (d, J = 7.2 Hz, 6H). ^{13}C NMR (100 MHz, MeOD) 142.9, 139.5, 132.4, 129.7, 129.33, 129.30, 127.7, 119.7, 105.5, 71.9, 69.2, 62.7, 34.5, 23.1, 22.7, 12.4. ESI-MS: 364.33. UPLC: 4.88 min.

*3-Benzyl-2-(3,3-dimethylbut-1-yn-1-yl)-9-methyl-4H,6H-thieno-[2,3-e][1,2,4]triazolo[3,4-c][1,4]oxazepine (**13**).* ^{1}H NMR (400 MHz, MeOD) δ = 7.32−7.23 (m, 2H), 7.23−7.17 (m, 3H), 4.71 (s, 2H), 4.70 (s, 2H), 4.00 (s, 2H), 2.75 (s, 3H), 1.32 (s, 9H). ^{13}C NMR (100 MHz, MeOD) 142.9, 139.6, 132.4, 129.7, 129.3, 129.1, 127.7, 119.6, 108.4, 71.5, 69.2, 62.7, 34.5, 31.0, 29.6, 12.4. ESI-MS: 378.38. UPLC: 5.24 min.

*3-Benzyl-2-(cyclopropylethynyl)-9-methyl-4H,6H-thieno[2,3-e]-[1,2,4]triazolo[3,4-c][1,4]oxazepine (**14**).* ^{1}H NMR (400 MHz, MeOD) δ = 7.32−7.23 (m, 2H), 7.23−7.15 (m, 3H), 4.69 (s, 2H), 4.67 (s, 2H), 4.00 (s, 2H), 2.74 (s, 3H), 1.62−1.51 (m, 1H), 1.02−0.91 (m, 2H), 0.81−0.73 (m, 2H). ^{13}C NMR (100 MHz, MeOD) 155.4, 153.0, 143.1, 139.6, 132.2, 129.7, 129.3, 127.7, 119.8, 103.8, 69.0, 67.4, 62.7, 34.5, 12.4, 9.6, 1.0. ESI-MS: 362.40. UPLC: 4.77 min.

*3-Benzyl-2-(cyclobutylethynyl)-9-methyl-4H,6H-thieno[2,3-e]-[1,2,4]triazolo[3,4-c][1,4]oxazepine (**15**).* ^{1}H NMR (400 MHz, MeOD) δ = 7.30−7.22 (m, 2H), 7.24−7.14 (m, 3H), 4.70 (s, 2H), 4.69 (s, 2H), 4.00 (s, 2H), 3.33−3.28 (m, 1H), 2.76 (s, 3H), 2.42−2.30 (m, 2H), 2.26−2.12 (m, 2H), 2.25−1.90 (m, 2H), ESI-MS: 376.42. UPLC: 5.41 min.

*3-Benzyl-2-(cyclopentylethynyl)-9-methyl-4H,6H-thieno[2,3-e]-[1,2,4]triazolo[3,4-c][1,4]oxazepine (**16**).* ^{1}H NMR (400 MHz, MeOD) δ = 7.31−7.22 (m, 2H), 7.21−7.15 (m, 3H), 4.70 (s, 2H), 4.68 (s, 2H), 4.00 (s, 2H), 2.97−2.90 (m, 1H), 2.75 (s, 3H), 2.05−1.96 (m, 2H), 1.80−1.58 (m, 6H). ^{13}C NMR (100 MHz, MeOD) 155.4, 153.1, 142.8, 139.6, 132.3, 129.7, 129.3, 129.0, 127.7, 119.9, 104.7, 72.2, 69.1, 62.7, 34.8, 34.5, 32.2, 25.9, 12.4. ESI-MS: 390.37. UPLC: 5.50 min.

*3-Benzyl-2-(cyclohexylethynyl)-9-methyl-4H,6H-thieno[2,3-e]-[1,2,4]triazolo[3,4-c][1,4]oxazepine (**17**).* ^{1}H NMR (400 MHz, MeOD) δ = 7.32−7.28 (m, 2H), 7.23−7.15 (m, 3H), 4.70 (s, 2H), 4.68 (s, 2H), 4.03 (s, 2H), 2.77−2.68 (m, 1H), 2.74 (s, 3H), 1.91−1.86 (m, 2H), 1.78−1.67 (m, 2H), 1.61−1.48 (m, 3H), 1.46−1.34 (m, 3H). ^{13}C NMR (100 MHz, MeOD) 155.3, 153.1, 142.9, 139.6, 132.3, 129.7, 129.32, 129.28, 127.7, 119.7, 104.3, 72.9, 69.1, 62.7, 34.5, 33.5, 31.0, 26.9, 25.6, 12.4. ESI-MS: 404.48. UPLC: 6.40 min.

*3-Benzyl-9-methyl-2-(piperidin-4-ylethynyl)-4H,6H-thieno[2,3-e][1,2,4]triazolo[3,4-c][1,4]oxazepine (**18**).* ^{1}H NMR (400 MHz, DMSO) δ = 7.35−7.27 (m, 2H), 7.25−7.17 (m, 3H), 4.74 (s, 2H), 4.69 (s, 2H), 3.99 (s, 2H), 3.22−3.15 (m, 2H), 3.12−2.97 (m, 3H), 2.73 (s, 3H), 2.66 (brs, 1H), 2.08−2.01 (m, 2H), 1.82−1.69 (m, 2H). ESI-MS: 405.23. UPLC: 2.3 min.

*3-Benzyl-9-methyl-2-((1-methylpiperidin-4-yl)ethynyl)-4H,6H-thieno[2,3-e][1,2,4]triazolo[3,4-c][1,4]oxazepine (**19**).* ^{1}H NMR (400 MHz, MeOD) δ = 7.36−7.22 (m, 2H), 7.22−7.15 (m, 3H), 4.70 (s, 2H), 4.67 (s, 2H), 4.04 (s, 2H), 3.57−3.50 (m, 2H), 3.09−2.93 (m, 3H), 2.87 (s, 3H), 2.72 (s, 3H), 2.09−2.01 (m, 2H), 1.96−1.83 (m, 2H). ESI-MS: 419.51. UPLC: 1.77 min.

*3-Benzyl-9-methyl-2-((tetrahydro-2H-pyran-4-yl)ethynyl)-4H,6H-thieno[2,3-e][1,2,4]triazolo[3,4-c][1,4]oxazepine (**20**).* ^{1}H NMR (400 MHz, MeOD) δ = 7.32−7.24 (m, 2H), 7.23−7.16 (m, 3H), 4.71 (s, 2H), 4.69 (s, 2H), 4.04 (s, 2H), 3.89−3.80 (m, 2H), 3.58−3.48 (m, 2H), 3.03−2.93 (m, 1H), 2.76 (s, 3H), 1.95−1.85 (m, 2H), 1.75−1.62 (m, 2H). ^{13}C NMR (100 MHz, MeOD) 155.4, 153.1, 143.3, 139.4, 132.4, 129.8, 129.5, 129.2, 127.7, 119.2, 102.4, 73.6, 69.2, 67.2, 62.7, 34.5, 33.1, 28.2, 12.4. ESI-MS: 406.40. UPLC: 4.27 min.

*3-Benzyl-9-methyl-2-((1-methyl-1H-imidazol-5-yl)ethynyl)-4H,6H-thieno[2,3-e][1,2,4]triazolo[3,4-c][1,4]oxazepine (**21**).* ^{1}H NMR (400 MHz, MeOD) δ = 7.32−7.24 (m, 2H), 7.23−7.16 (m, 3H), 4.71 (s, 2H), 4.69 (s, 2H), 4.04 (s, 2H), 3.89−3.80 (m, 2H), 3.58−3.48 (m, 2H), 3.03−2.93 (m, 1H), 2.76 (s, 3H), 1.95−1.85 (m, 2H), 1.75−1.62 (m, 2H). ^{13}C NMR (100 MHz, MeOD) 155.4, 153.1, 143.3, 139.4, 132.4, 129.8, 129.5, 129.2, 127.7, 119.2, 102.4, 73.6, 69.2, 67.2, 62.7, 34.5, 33.1, 28.2, 12.4. ESI-MS: 406.40. UPLC: 4.27 min.

*3-Benzyl-9-methyl-2-((1-methyl-1H-pyrazol-4-yl)ethynyl)-4H,6H-thieno[2,3-e][1,2,4]triazolo[3,4-c][1,4]oxazepine (**22**).* ^{1}H NMR (400 MHz, MeOD) δ = 7.87 (s, 1H), 7.63 (s, 1H), 7.32−7.24 (m, 2H),

DOI: 10.1021/acs.jmedchem.8b00506
J. Med. Chem. XXXX, XXX, XXX−XXX

7.24−7.16 (m, 3H), 4.70 (s, 2H), 4.68 (s, 2H), 4.07 (s, 2H), 3.89 (s, 3H), 2.73 (s, 3H). ^{13}C NMR (100 MHz, MeOD) 141.9, 141.4, 138.2, 133.8, 130.7, 129.4, 128.4, 127.9, 126.3, 117.5, 102.0, 88.5, 80.2, 67.5, 61.4, 37.8, 33.3, 11.1. ESI-MS: 402.38. UPLC: 3.27 min.

*3-Benzyl-9-methyl-2-(pyridin-4-ylethynyl)-4H,6H-thieno[2,3-e]-[1,2,4]triazolo[3,4-c][1,4]oxazepine (**23**).* ^{1}H NMR (400 MHz, MeOD) δ 8.77 (d, J = 6.4 Hz, 1H), 7.98 (d, J = 6.4 Hz, 1H), 7.31 (dd, J = 8.0 Hz, J = 7.2 Hz, 2H), 7.29−7.19 (m, 3H), 4.78−4.73 (m, 4H), 4.23 (s, 2H), 2.79 (s, 3H). ESI-MS: M + H 399.41. UPLC: 3.52 min.

*3-Benzyl-9-methyl-2-(pyridin-3-ylethynyl)-4H,6H-thieno[2,3-e]-[1,2,4]triazolo[3,4-c][1,4]oxazepine (**24**).* ^{1}H NMR (400 MHz, MeOD) δ 8.88−8.66 (m, 2H), 8.25 (d, J = 8.0 Hz, 1H), 7.76−7.70 (m, 1H), 7.31 (dd, J = 7.4 Hz, J = 7.3 Hz, 2H), 7.27−7.18 (m, 3H), 4.76 (s, 2H), 4.75 (s, 2H), 4.18 (s, 2H), 2.80 (s, 3H). ESI-MS: M + H 399.44. UPLC: 3.50 min.

*3-Benzyl-9-methyl-2-(pyridin-2-ylethynyl)-4H,6H-thieno[2,3-e]-[1,2,4]triazolo[3,4-c][1,4]oxazepine (**25**).* ^{1}H NMR (400 MHz, MeOD) δ = 8.57 (d, J = 5.2 Hz, 1H), 7.89 (dd, J = 7.6 Hz, J = 8.0 Hz, 1H), 7.64 (d, J = 7.6 Hz, 1H), 7.44 (dd, J = 7.6 Hz, J = 7.6 Hz, 1H), 7.35−7.17 (m, 5H), 4.73 (s, 2H), 4.72 (s, 2H), 4.20 (s, 2H), 2.76 (s, 3H), ESI-MS: 399.31. UPLC: 3.44 min.

*4-(4-((3-Benzyl-9-methyl-4H,6H-thieno[2,3-e][1,2,4]triazolo[3,4-c][1,4]oxazepin-2-yl)ethynyl)-1H-pyrazol-1-yl)-2-(2,6-dioxopiperidin-3-yl)isoindoline-1,3-dione (**26**).* 4-Ethynyl-1*H*-pyrazole (9.2 mg, 2 equiv), $Pd(PPh_3)_2Cl_2$ (4.2 mg), CuI (2.3 mg), THF (1 mL), and Et_3N (1 mL) were added under N_2 to a flask charged with **47** (20 mg, 0.05 mmol). The reaction mixture was stirred at 60 °C for 8 h. The reaction mixture was extracted with EtOAc, and the organic layer was washed with brine, dried, and concentrated. The residue was purified through HPLC to afford 2-((1*H*-pyrazol-4-yl)ethynyl)-3-benzyl-9-methyl-4*H*,6*H*-thieno[2,3-*e*][1,2,4]triazolo[3,4-*c*][1,4]oxazepine (**48**) in 70% yield. ^{1}H NMR (400 MHz, DMSO-d_6) δ = 13.3 (brs, 1H), 8.19 (s, 1H), 7.78 (s, 1H), 7.32 (dd, J = 7.6 Hz, J = 7.2 Hz, 2H), 7.28−7.17 (m, 3H), 4.71 (s, 2H), 4.69 (s, 2H), 4.04 (s, 2H), 2.65 (s, 3H). ^{13}C NMR (100 MHz, DMSO-d_6) 163.1, 150.6, 141.7, 138.4, 129.74, 129.65, 128.8, 128.3, 126.6, 115.8, 100.3, 89.7, 80.8, 67.6, 62.0, 33.3, 12.3. ESI-MS: 388.22.

2-(2,6-Dioxopiperidin-3-yl)-4-fluoroisoindoline-1,3-dione (**49**) (14 mg, 1 equiv), Et_3N (0.1 mL), and DMSO (2 mL) were added to a flask charged with compound **48** (20 mg, 0.05 mmol). The reaction mixture was stirred at 120 °C for 8 h. The reaction mixture was extracted with EtOAc, and the organic layer was washed with brine, dried. and concentrated. The residue was purified through HPLC to afford compound **26** (20% yield).

*4-((4-((3-Benzyl-9-methyl-4H,6H-thieno[2,3-e][1,2,4]triazolo[3,4-c][1,4]oxazepin-2-yl)ethynyl)-1H-pyrazol-1-yl)methoxy)-2-(2,6-dioxopiperidin-3-yl)isoindoline-1,3-dione (**27**).* Compound **51** 2-(2,6-dioxopiperidin-3-yl)-4-hydroxyisoindoline-1,3-dione (274 mg, 1.0 mmol) in DMF (2 mL) was added to a solution of compound **50** (1*H*-pyrazol-1-yl) methylmethanesulfonate (193 mg, 1.1 mmol $KHCO_3$ (200 mg) and KI (10 mg). The reaction mixture was stirred at 90 °C for 12 h prior to being taken up in EtOAc and H_2O. The organic layer was separated, dried, and evaporated. The residue was purified by chromatography to afford 4-((1*H*-pyrazol-1-yl)methoxy)-2-(2,6-dioxopiperidin-3-yl)isoindoline-1,3-dione **52** (180 mg, 51%). ESI-MS: 355.12.

N-Iodosuccinimide (113 mg) was added to a solution of **52** (180 mg, 0.5 mmol) in AcOH (2 mL). The reaction was stirred for 1 h prior to being concentrated. The residue was purified by HPLC to afford 2-(2,6-dioxopiperidin-3-yl)-4-((4-iodo-1*H*-pyrazol-1-yl)methoxy)-isoindoline-1,3-dione (**53**). ESI-MS: 481.02.

CuI (1 mg), $Pd(Ph_3P)_2Cl_2$ (3.5 mg), **53** (33 mg, 0.069 mmol), ethynyltrimethylsilane (20 mg), THF (2 mL) and Et_3N (0.5 mL) were placed in a Schlenk tube. The reaction mixture was heated at 50 °C for 12 h. The reaction mixture was cooled and treated with EtOAc and brine. The organic layer was separated, dried, and evaporated. The residue was purified by chromatography (DCM/MeOH 9:1) to afford crude product, which was dissolved in THF, and a solution of TBAF in THF (1M, 0.1 mL) was added. After 5 min, the reaction mixture was evaporated, and the residue was purified by HPLC to afford 2-(2,6-dioxopiperidin-3-yl)-4-((4-ethynyl-1*H*-pyrazol-1-yl)methoxy)-isoindoline-1,3-dione (**54**) (17 mg, 65%). ESI-MS: 379.12.

CuI (0.45 mg), $Pd_2(dba)_3$ (1.38 mg), $HP^tBu_3BF_4$ (1.39 mg), **54** (19 mg, 0.05 mmol), **47** (10 mg, 0.03 mmol), THF(2 mL), and HN^iPr_2 (0.1 mL) were placed in a Schlenk tube. The reaction mixture was heated at 60−70 °C for 12 h. The reaction mixture was cooled and treated with EtOAc and brine. The organic layer was separated, dried, and evaporated. The residue was purified by HPLC to afford compound **27** (6.5 mg, 32% yield). ^{1}H NMR (400 MHz, MeOD) δ = 8.19 (s, 1H), 7.91 (s, 1H), 7.79−7.73 (m, 1H), 7.71 (s, 1H), 7.70−7.56 (m, 2H), 7.30−7.26 (m, 2H), 7.23−7.16 (m, 3H), 6.29 (s, 2H), 5.15−5.04 (m, 1H), 4.71 (s, 2H), 4.69 (s, 2H), 4.08 (s, 2H), 2.77−2.64 (m, 2H), 2.74 (s, 3H), 2.16−2.06 (m, 2H). ESI-MS: 674.22.

*General Procedure for Synthesis of Compounds **28**−**31**.* MsCl (1 mL, 12.6 mmol) was added at 0 °C to a solution of compound **55** 4-iodo-1*H*-pyrazole (2.4 g, 12 mmol) and triethylamine (1.85 mL, 13 mmol) in DCM (20 mL). The reaction mixture was allowed to warm to r.t. and stirred further for a 1 h. The reaction mixture was quenched with a saturated NH_4Cl solution and extracted with DCM. The organic layer was separated, washed with brine, dried, and evaporated. The residue was dissolved in CH_3CN (70 mL), and *tert*-butyl(4-hydroxybutyl) carbamate (1.89 g, 10 mmol) and Cs_2CO_3 (3.9 g, 12 mmol) were added. The reaction mixture was heated to reflux for 12 h. After the reaction was cooled, the mixture was filtered, and the filtrate was evaporated. The residue was taken up in EtOAc and H_2O. The organic layer was separated, washed with brine, dried, and evaporated. The residue was purified by chromatography (EtOAc/hexanes:1:2) to afford crude *tert*-butyl(4-(4-iodo-1*H*-pyrazol-1-yl)butyl)carbamate (2.3 g, 53%), which was treated with DCM (5 mL) and TFA (5 mL). This reaction mixture was stirred for 12 h. All the volatiles were removed under vacuum, and the residue was subject to HPLC purification to afford 4-(4-iodo-1*H*-pyrazol-1-yl)butan-1-amine (**56**).

DIPEA (0.52 mL, 3 mmol) was added to a solution of the TFA salt of compound **56** (378 mg, 1 mmol) and 2-(2, 6-dioxopiperidin-3-yl)-4-fluoroisoindoline-1,3-dione (276 mg, 1 mmol) in DMF (1 mL). The reaction mixture was heated at 90 °C for 12 h. The reaction mixture was cooled and treated with EtOAc and brine. The organic layer was separated, dried, and evaporated. The residue was subject to HPLC purification to afford compound **57**, 2-(2, 6-dioxopiperidin-3-yl)-4-((4-(4-iodo-1*H*-pyrazol-1-yl)butyl)amino)isoindoline-1,3-dione (122 mg, 23% yield).

CuI (5.3 mg), $Pd(Ph_3P)_2Cl_2$ (20 mg), compound **57** (100 mg, 0.2 mmol), ethynyltrimethylsilane (39.2 mg, 0.4 mmol), THF (4 mL), and Et_3N (1 mL) were placed in a Schlenk tube. The reaction mixture was heated at 60 °C for 12 h and then cooled and treated with EtOAc and brine. The organic layer was separated, dried, and evaporated. The residue was purified by chromatography (EtOAc) to afford crude product, which was dissolved in THF, and a solution of TBAF in THF (1 M, 0.2 mL) was added. After 5 min, the reaction mixture was evaporated, and the residue was subjected to HPLC purification to afford 2-(2,6-dioxopiperidin-3-yl)-4-((4-(4-ethynyl-1*H*-pyrazol-1-yl)-butyl)-amino)isoindoline-1,3-dione (**58**) (50 mg, 60% yield). ESI-MS: 420.13.

CuI (3.8 mg), $Pd(Ph_3P)_2Cl_2$ (7 mg), compound **58** (20 mg, 0.05 mmol), compound **47** (42 mg, 0.1 mmol), THF (2 mL), and Et_3N (0.5 mL) were placed in a Schlenk tube. The reaction mixture was heated at 70 °C for 12 h. The reaction mixture was cooled and treated with EtOAc and brine. The organic layer was separated, dried, and evaporated. The residue was subjected to HPLC purification to afford compound **30**. Following the procedures used to prepare compound **30** from *tert*-butyl(4-hydroxybutyl) carbamate, compounds **28**, **29**, and **31** with different alkynyl chains were obtained with the same methods.

*4-((2-(4-((3-Benzyl-9-methyl-4H,6H-thieno[2,3-e][1,2,4]triazolo-[3,4-c][1,4]oxazepin-2-yl)ethynyl)-1H-pyrazol-1-yl)ethyl)amino)-2-(2,6-dioxopiperidin-3-yl)isoindoline-1,3-dione (**28**).* ^{1}H NMR (400 MHz, $CDCl_3$) δ = 7.97 (brs, 1H), 7.71 (s, 1H), 7.58 (s, 1H), 7.46 (dd, J = 7.0 Hz, J = 7.8 Hz, 1H), 7.30 (dd, J = 6.8 Hz, J = 7.2 Hz, 1H), 7.23 (d, J = 6.8 Hz, 1H), 7.18 (d, J = 7.2 Hz, 1H), 7.12 (d, J = 7.0 Hz, 1H), 6.76 (d, J = 7.8 Hz, 1H), 6.49 (s, 1H), 4.94−4.83 (m, 1H), 4.73 (s, 2H), 4.60 (s,

DOI: 10.1021/acs.jmedchem.8b00506
J. Med. Chem. XXXX, XXX, XXX−XXX

2H), 4.35 (t, J = 5.8 Hz, 2H), 4.02 (s, 2H), 3.83−2.76 (m, 2H), 2.79−2.66 (m, 4H), 2.73 (s, 3H). ESI-MS: 687.37. UPLC: 3.74 min.

*4-((3-(4-((3-Benzyl-9-methyl-4H,6H-thieno[2,3-e][1,2,4]triazolo-[3,4-c][1,4]oxazepin-2-yl)ethynyl)-1H-pyrazol-1-yl)propyl)amino)-2-(2,6-dioxopiperidin-3-yl)isoindoline-1,3-dione (**29**).* ^{1}H NMR (400 MHz, $CDCl_3$) δ = 7.97 (brs, 1H), 7.71 (s, 1H), 7.58 (s, 1H), 7.46 (dd, J = 7.0 Hz, J = 7.8 Hz, 1H), 7.30 (dd, J = 6.8 Hz, J = 7.2 Hz, 1H), 7.23 (d, J = 6.8 Hz, 1H), 7.18 (d, J = 7.2 Hz, 1H), 7.12 (d, J = 7.0 Hz, 1H), 6.76 (d, J = 7.8 Hz, 1H), 6.49 (s, 1H), 4.94−4.83 (m, 1H), 4.73 (s, 2H), 4.60 (s, 2H), 4.35 (t, J = 5.8 Hz, 2H), 4.02 (s, 2H), 3.83−2.76 (m, 2H), 2.79−2.66 (m, 4H), 2.73 (s, 3H). ESI-MS: 701.40. UPLC: 4.01 min.

*4-((4-(4-((3-Benzyl-9-methyl-4H,6H-thieno[2,3-e][1,2,4]triazolo-[3,4-c][1,4]oxazepin-2-yl)ethynyl)-1H-pyrazol-1-yl)butyl)amino)-2-(2,6-dioxopiperidin-3-yl)isoindoline-1,3-dione (**30**).* ^{1}H NMR (400 MHz, DMSO-d_6) δ = 11.09 (brs, 1H), 8.19 (s, 1H), 7.75 (s, 1H), 7.55 (dd, J = 7.2 Hz, J = 6.8 Hz, 1H), 7.31 (dd, J = 7.6 Hz, J = 7.2 Hz, 2H), 7.27−7.15 (m, 3H), 7.08 (d, J = 8.4 Hz, 1H), 7.00 (d, J = 6.8 Hz, 1H), 6.61 (brs, 1H), 5.08−5.00 (m, 1H), 4.71 (s, 2H), 4.69 (s, 2H), 4.17 (t, J = 6.8 Hz, 2H), 4.03 (s, 2H), 2.94−2.81 (m, 1H), 2.65 (s, 3H), 2.65−2.50 (m, 2H), 2.50−2.43 (m, 2H), 2.05−1.97 (m, 2H), 1.90−1.79 (m, 2H), 1.55−1.44 (m, 2H). ^{13}C NMR (100 MHz, DMSO-d_6) 172.9, 170.2, 168.9, 167.4, 115.1, 150.6, 146.4, 141.8, 141.5, 138.3, 136.3, 133.7, 132.3, 129.8, 129.7, 128.8, 128.3, 126.6, 117.3, 115.7, 110.5, 109.2, 100.6, 89.3, 80.8, 67.6, 62.0, 51.2, 48.6, 41.3, 33.3, 31.1, 27.0, 25.7, 22.2, 12.3. ESI-MS: 715.39. UPLC: 4.31 min.

*4-((5-(4-((3-Benzyl-9-methyl-4H,6H-thieno[2,3-e][1,2,4]triazolo-[3,4-c][1,4]oxazepin-2-yl)ethynyl)-1H-pyrazol-1-yl)pentyl)amino)-2-(2,6-dioxopiperidin-3-yl)isoindoline-1,3-dione (**31**).* ^{1}H NMR (400 MHz, $CDCl_3$) δ = 8.23 (brs, 1H), 7.71 (s, 1H), 7.61 (s, 1H), 7.48 (dd, J = 7.2 Hz, J = 6.8 Hz, 1H), 7.33 (dd, J = 7.2 Hz, J = 7.6 Hz, 2H), 7.23 (d, J = 7.6 Hz, 1H), 7.18 (d, J = 6.8 Hz, 2H), 7.09 (d, J = 6.8 Hz, 1H), 6.85 (d, J = 8.4 Hz, 1H), 4.95−4.83 (m, 1H), 4.80 (s, 2H), 4.68 (s, 2H), 4.17 (t, J = 7.0 Hz, 2H), 4.04 (s, 2H), 3.30−3.20 (m, 2H), 2.95−2.65 (m, 3H), 2.88 (s, 3H), 2.19−2.05 (m, 1H), 2.00−1.85 (m, 2H), 1.78−1.61 (m, 2H), 1.50−1.33 (m, 2H). ESI-MS: 729.40. UPLC: 4.33 min.

*General Procedure for Synthesis of Compounds **32** and **33**.* Compound **60**, 4-chlorobutan-1-ol (3.3 g, 1.3eq), Cs_2CO_3 (16.4 g, 60 mmol), and NaI (600 mg) were added to a solution of compound **59** and 4-iodo-1*H*-pyrazole (3.88 g, 20 mmol) in CH_3CN (140 mL). The reaction mixture was heated at 50 °C for 12 h. The reaction mixture was filtered, and the filtrate was evaporated. The residue was purified by chromatography (EtOAc/hexanes 1:1 to EtOAc) to afford compound **61**, 4-(4-iodo-1*H*-pyrazol-1-yl) butan-1-ol (4 g, 75%).

The SO_3·pyridine complex (7.1 g, 45 mmol) was added to a solution of compound **61** (4 g, 15 mmol) in DMSO (24 mL) and Et_3N (16 mL). The reaction mixture was stirred for 3 h prior to being quenched with H_2O. The reaction mixture was extracted with EtOAc. The organic layer was separated, washed with brine, dried, and evaporated. The residue was purified by chromatography (EtOAc/hexanes: 1:2 to EtOAc) to afford compound **62**, 4-(4-iodo-1*H*-pyrazol-1-yl)butanal (2.8 g, 73%). ^{1}H NMR (400 MHz, $CDCl_3$) δ 9.76 (s, 1H), 7.52 (s, 1H), 7.44 (s, 1H), 4.20 (t, J = 6.7 Hz, 2H), 2.48 (t, J = 6.9 Hz, 2H), 2.18−2.10 (m, 2H).

AcOH (0.06 mL) was added to a solution of compound **62** (526 mg, 2 mmol) and compound **63** (lenalidomide) (520 mg, 2 mmol) in DCE (20 mL). The reaction was stirred for 20 min prior to the addition of $NaHB(OAc)_3$ (848 mg). The reaction mixture was stirred for 12 h prior to being quenched with H_2O. The reaction mixture was extracted with DCM. The organic layer was separated, washed with brine, dried, and evaporated. The residue was purified by HPLC to afford 3-(4-((4-(4-iodo-1*H*-pyrazol-1-yl)butyl)amino)-1-oxoisoindolin-2-yl)piperidine-2,6-dione (**64**) (420 mg, 38%). ^{1}H NMR (400 MHz, MeOD) δ 7.73−7.70 (m, 1H), 7.50−7.45 (m, 1H), 7.32−7.25 (m, 1H), 7.10−7.05 (m, 1H), 6.80−6.75 (m, 1H), 5.16−5.06 (m, 1H), 4.28−4.20 (m, 2H), 4.22−4.12 (m, 2H), 3.24−3.20 (m, 2H), 2.84−2.80 (m, 2H), 2.48−2.40 (m, 1H), 2.20−2.15 (m, 1H), 1.99−1.89 (m, 2H), 1.63−1.58 (m, 2H). ESI-MS: 508.95.

CuI (9.5 mg), $Pd(Ph_3P)_2Cl_2$ (35 mg), compound **64** (267 mg, 0.5 mmol), ethynyltrimethylsilane (98 mg, 1 mmol), THF (4 mL), and Et_3N (1 mL) were placed in a Schlenk tube. The reaction mixture was heated at 40 °C for 12 h, then cooled and treated with EtOAc and brine. The organic layer was separated, dried, and evaporated. The residue was purified by chromatography (EtOAc) to afford crude product (215 mg, 90%), which was dissolved in THF, and a solution of TBAF in THF (1 M, 0.45 mL) was added. After 5 min, the reaction mixture was evaporated, and the residue was purified by chromatography (EtOAc) to afford crude product, which was further purified by HPLC to afford 3-(4-((4-(4-ethynyl-1*H*-pyrazol-1-yl)butyl)amino)-1-oxoisoindolin-2-yl)piperidine-2,6-dione compound (**65**) (100 mg, 55% yield). ESI-MS: 406.24.

CuI (1.9 mg), $Pd_2(dba)_3$ (18.3 mg), $HP^tBu_3BF_4$ (11.6 mg), compound **65** (81 mg, 0.2 mmol), compound **47** (39 mg, 0.1 mmol), THF (4 mL), and HN^iPr_2 (0.14 mL) were placed in a Schlenk tube. The reaction mixture was heated at 40 °C for 12 h. The reaction mixture was cooled and treated with EtOAc and brine. The organic layer was separated, dried, and evaporated. The residue was purified by HPLC to afford compound **33**. Following the procedures used to prepare compound **33** from 4-chlorobutan-1-ol, compounds **32** with different alkynyl chains were obtained with the same methods.

*3-(4-((3-(4-((3-Benzyl-9-methyl-4H,6H-thieno[2,3-e][1,2,4]-triazolo[3,4-c][1,4]oxazepin-2-yl)ethynyl)-1H-pyrazol-1-yl)propyl)-amino)-1-oxoisoindolin-2-yl)piperidine-2,6-dione (**32**).* ^{1}H NMR (400 MHz, DMSO-d_6) δ = 11.01 (brs, 1H), 8.21 (s, 1H), 7.77 (s, 1H), 7.31 (dd, J = 7.2 Hz, J = 7.2 Hz, 2H), 7.30−7.18 (m, 4H), 6.94 (d, J = 6.8 Hz, 1H), 6.70 (d, J = 7.6 Hz, 1H), 6.53 (brs, 1H), 5.15−5.07 (m, 1H), 4.71 (s, 2H), 4.69 (s, 2H), 4.25 (t, J = 7.0 Hz, 2H), 4.22−4.08 (m, 2H), 4.03 (s, 2H), 3.15−3.06 (m, 2H), 2.65 (s, 3H), 2.68−2.55 (m, 1H), 2.14−2.05 (m, 2H). ESI-MS: 687.42. UPLC: 3.59 min.

*3-(4-((4-(4-((3-Benzyl-9-methyl-4H,6H-thieno[2,3-e][1,2,4]-triazolo[3,4-c][1,4]oxazepin-2-yl)ethynyl)-1H-pyrazol-1-yl)butyl)-amino)-1-oxoisoindolin-2-yl)piperidine-2,6-dione (**33**).* ^{1}H NMR (400 MHz, MeOD) δ = 7.93 (s, 1H), 7.66 (s, 1H), 7.33−7.25 (m, 2H), 7.22−7.16 (m, 3H), 7.06 (d, J = 7.2 Hz, 1H), 6.79 (d, J = 8.0 Hz, 1H), 5.19−5.10 (m, 1H), 4.71 (s, 2H), 4.69 (s, 2H), 4.27 (t, J = 4.0 Hz, 2H), 4.23−4.18 (m, 2H), 4.08 (s, 2H), 3.16−3.11 (m, 2H), 2.74 (s, 3H), 2.53−2.38 (m, 2H), 2.22−2.11 (m, 2H), 2.05−1.92 (m, 2H), 1.67−1.55 (m, 2H). ESI-MS: 701.43. UPLC: 3.79 min.

*3-(4-(5-(4-((3-Benzyl-9-methyl-4H,6H-thieno[2,3-e][1,2,4]-triazolo[3,4-c][1,4]oxazepin-2-yl)ethynyl)-1H-pyrazol-1-yl)pentyl)-1-oxoisoindolin-2-yl)piperidine-2,6-dione (**34**).* CuI (5.3 mg), Pd-$(Ph_3P)_2Cl_2$ (20 mg), compound **66** 3-(4-bromo-1-oxoisoindolin-2-yl)piperidine-2,6-dione (100 mg, 0.31 mmol), 1-(pent-4-yn-1-yl)-1*H*-pyrazole (50 mg, 0.37 mmol), DMF (4 mL), and Et_3N (1 mL) were placed in a Schlenk tube. The reaction mixture was heated at 80 °C for 12 h. The reaction mixture was cooled and treated with EtOAc and brine. The organic layer was separated, dried, and evaporated. The residue was purified by chromatography (MeOH/DCM) to afford the desired product (**67**), 3-(4-(5-(1*H*-pyrazol-1-yl)pent-1-yn-1-yl)-1-oxoisoindolin-2-yl)piperidine-2,6-dione (82 mg, 70% yield). ESI-MS: 377.15.

Ten percent Pd/C was added to a solution of the compound **67** (100 mg, 0.266 mmol) in MeOH (2 mL). The reaction was stirred under an H_2 balloon for 4 h and then filtered. The organic solvent was removed to afford compound **68**, 3-(4-(5-(1*H*-pyrazol-1-yl)pentyl)-1-oxoisoindolin-2-yl)piperidine-2,6-dione (97 mg, 95%).

NIS (56 mg) was added to compound **68** (100 mg, 0.26 mmol) in acetic acid (2 mL). The reaction was stirred for 6 h prior to being concentrated. The residue was purified by HPLC to afford compound **69** 3-(4-(5-(4-iodo-1*H*-pyrazol-1-yl)pentyl)-1-oxoisoindolin-2-yl)-piperidine-2,6-dione (118 mg, 90%). ESI-MS: 507.19.

CuI (5.3 mg), $Pd(Ph_3P)_2Cl_2$ (20 mg), compound **69** (101 mg, 0.2 mmol), ethynyltrimethylsilane (39.2 mg, 0.4 mmol), THF (4 mL), and Et_3N (1 mL) were placed in a Schlenk tube. The reaction mixture was heated at 70 °C for 12 h. The reaction mixture was cooled and treated with EtOAc and brine. The organic layer was separated, dried, and evaporated. The residue was purified by chromatography (EtOAc) to afford a crude product, which was dissolved in THF, and a solution of TBAF in THF (1 M, 0.2 mL) was added. After 5 min, the reaction mixture was evaporated, and the residue was subjected to HPLC purification to afford compound **70**, 3-(4-(5-(4-ethynyl-1*H*-pyrazol-1-

DOI: 10.1021/acs.jmedchem.8b00506
J. Med. Chem. XXXX, XXX, XXX−XXX

yl)pentyl)-1-oxoisoindolin-2-yl)piperidine-2,6-dione (44 mg, 55% yield). ESI-MS: 405.19.

CuI (3.8 mg), $Pd(Ph_3P)_2Cl_2$ (7 mg), compound **47** (20 mg, 0.05 mmol), compound **70** (40 mg, 0.1 mmol), THF (2 mL), and Et_3N (0.5 mL) were placed in a Schlenk tube. The reaction mixture was heated at 70 °C for 12 h. The reaction mixture was cooled and treated with EtOAc and brine. The organic layer was separated, dried, and evaporated. The residue was subjected to HPLC purification to afford compound **34** (35.7 mg, 55% yield). ^{1}H NMR (400 MHz, $CDCl_3$) δ = 8.01 (brs, 1H), 7.74 (d, J = 7.6 Hz, 1H), 7.68 (s, 1H), 7.58 (s, 1H), 7.43 (dd, J = 7.2 Hz, J = 7.6 Hz, 1H), 7.40−7.34 (m, 2H), 7.32 (dd, J = 7.6 Hz, J = 6.8 Hz, 2H), 7.18 (d, J = 7.6 Hz, 1H), 5.33−5.22 (m, 1H), 4.79 (s, 2H), 4.67 (s, 2H), 4.49−4.22 (m, 2H), 4.14 (t, J = 7.0 Hz, 2H), 4.05 (s, 2H), 2.93−2.73 (m, 4H), 2.86 (s, 3H), 2.69−2.55 (m, 1H), 1.97−1.83 (m, 2H), 1.75−1.62 (m, 2H), 1.49−1.23 (m, 2H). ESI-MS: 700.40. UPLC: 5.43 min.

*3-(4-(5-(4-((3-Benzyl-9-methyl-4H,6H-thieno[2,3-e][1,2,4]-triazolo[3,4-c][1,4]oxazepin-2-yl)ethynyl)-1H-pyrazol-1-yl)pent-1-yn-1-yl)-1-oxoisoindolin-2-yl)piperidine-2,6-dione (**35**).* K_2CO_3 (4.0 mmol) was added to a solution of compound **48** (0.6 g, 1.55 mmol) and 5-iodopent-1-yne (776 mg, 4.0 mmol) in DMF (10 mL). The reaction mixture was stirred at 80 °C for 4 h. All volatiles were removed, and the residue was chromatographed on silica gel (DCM and MeOH) to afford compound **71**, 3-benzyl-9-methyl-2-((1-(pent-4-yn-1-yl)-1*H*-pyrazol-4-yl)ethynyl)-4*H*,6*H*-thieno[2,3-*e*][1,2,4]triazolo[3,4-*c*][1,4]-oxazepine (560 mg, 80%).

$Pd(PPh_3)_2Cl_2$ (0.124 mmol), CuI (0.062 mmol), and Et_3N (2.5 mL) were added to a solution of compound **71** (0.56 g, 1.24 mmol) and compound **72** 3-(4-iodo-1-oxoisoindolin-2-yl) piperidine-2,6-dione (600 mg, 1.62 mmol) in DMF (5 mL). The reaction mixture was degassed completely and stirred at 80 °C for 6 h. All volatiles were removed, and the residue was subjected to HPLC purification to afford the compound **35** (QCA570) (509 mg, 59% yield). ^{1}H NMR (400 MHz, DMSO-d_6) δ = 11.00 (brs, 1H), 8.23 (s, 1H), 7.75 (s, 1H), 7.71 (d, J = 7.6 Hz, 1H), 7.65 (d, J = 7.6 Hz, 1H), 7.51 (dd, J = 8.0 Hz, J = 7.6 Hz, 1H), 7.31 (dd, J = 7.6 Hz, J = 7.2 Hz, 2H), 7.26−7.17 (m, 3H), 5.18−5.10 (m, 1H), 4.72 (s, 2H), 4.69 (s, 2H), 4.53−4.30 (m, 2H), 4.28 (t, J = 5.8 Hz, 2H), 4.03 (s, 2H), 3.00−2.85 (m, 1H), 2.66 (s, 3H), 2.66−2.53 (m, 1H), 2.55−2.40 (m, 3H), 2.14−2.05 (m, 2H), 2.05−1.98 (m, 1H). ^{13}C NMR (100 MHz, DMSO-d_6) 172.9, 171.0, 167.7, 153.2, 150.6, 144.0, 141.8, 141.6, 138.3, 134.2, 133.9, 133.7, 132.0, 129.8, 128.8, 128.6, 128.3, 126.6, 122.8, 118.7, 115.7, 100.8, 94.9, 89.2, 80.8, 77.0, 67.6, 62.0, 51.7, 50.7, 47.1, 31.3, 28.7, 22.5, 16.2, 12.3. ESI-MS: 696.41. UPLC: 4.00 min.

*4-(5-(4-((3-Benzyl-9-methyl-4H,6H-thieno[2,3-e][1,2,4]triazolo-[3,4-c][1,4]oxazepin-2-yl)ethynyl)-1H-pyrazol-1-yl)pent-1-yn-1-yl)-2-(2,6-dioxopiperidin-3-yl)isoindoline-1,3-dione (**36**).* Obtained by the coupling of compound **71** with 2-(2,6-dioxopiperidin-3-yl)-4-iodoisoindoline-1,3-dione. The synthetic procedure is the same as that used for compound **35**. ^{1}H NMR (400 MHz, $CDCl_3$) δ 7.93 (s, 1H), 7.85 (s, 1H), 7.82 (d, J = 6.4 Hz, 1H), 7.77−7.66 (m, 3H), 7.33−7.25 (m, 2H), 7.17 (d, J = 7.6 Hz, 1H), 4.97 (dd, J = 12.0, 5.0 Hz, 1H), 4.77 (s, 2H), 4.64 (s, 2H), 4.56−4.48 (m, 2H), 4.04 (s, 2H), 2.89−2.70 (m, 6H), 2.50−2.43 (m, 2H), 2.25−2.17 (m, 4H). ESI-MS: 710.18.

*3-(4-(5-(4-((3-Benzyl-9-methyl-4H,6H-thieno[2,3-e][1,2,4]-triazolo[3,4-c][1,4]oxazepin-2-yl)ethynyl)-1H-pyrazol-1-yl)pent-1-yn-1-yl)-1-oxoisoindolin-2-yl)-1-methylpiperidine-2,6-dione (**37**).* Obtained by coupling of compound **71** with 3-(4-iodo-1-oxoisoindolin-2-yl)-1-methylpiperidine-2,6-dione. The synthetic procedure is the same as that used for compound **35**. ^{1}H NMR (400 MHz, $CDCl_3$) δ = 7.83 (d, J = 7.6 Hz, 1H), 7.66 (s, 1H), 7.63 (s, 1H), 7.57 (d, J = 6.8 Hz, 1H), 7.44 (dd, J = 7.6 Hz, J = 7.6 Hz, 1H), 7.30 (dd, J = 7.2 Hz, J = 7.6 Hz, 2H), 7.24 (d, J = 7.2 Hz, 1H), 7.18 (d, J = 7.6 Hz, 1H), 5.26−5.15 (m, 1H), 4.74 (s, 2H), 4.61 (s, 2H), 4.52−4.32 (m, 2H), 4.30 (t, J = 6.8 Hz, 2H), 4.04 (s, 2H), 3.19 (s, 3H), 3.06−2.77 (m, 4H), 2.75 (s, 3H), 2.48 (t, J = 7.0 Hz, 2H), 2.24−2.12 (m, 2H). ESI-MS: 710.40. UPLC: 4.37 min.

Molecular Modeling. The cocrystal structure of BRD4 BD1/(+)-JQ-1 (PDB entry: 3MXF)[11] was used to model the binding poses of compounds **2**, **3**, and **22** with BRD4 BD1. The chain A of BRD4 BD1 from the crystal structure was extracted, and the missing side chain of K141 was rebuilt using the MOE[56] program. For the amino acids where different conformations were determined, the rotamer A conformations were selected. Protons were then added to BRD4 BD1 using the "protonate 3D" module in MOE by setting at the pH 7.0 condition. All water molecules from the crystal structure were saved. Structures of the compounds were constructed and optimized using MOE. Fifteen binding poses of each compound to BRD4 BD1 were generated by the GOLD program (version 5.0.2)[57,58] in which the highest ranked pose was selected as the binding model for each compound. In the docking simulation, we set the binding site centered at F129 in BRD4 BD1 with a radius of 12 Å. In the binding site, water molecules W9, W12, W18, W15, W33, and W209 of BRD4 BD1 were included during the docking simulations with the flags on. PLP fitness function in Gold 5.0.2 was used to evaluate the docked poses, and default parameters for the genetic algorithm (GA) run were used. The top pose of each compound ranked by PLP was selected as its binding mode to BRD4 BD1. Figures were prepared using the PyMOL program (www.pymol.org).

Binding Affinities of Compounds to BET Proteins. Human BRD2 BD1 (residues 72−205), BRD2 BD2 (residues 349−460), BRD3 BD1 (residues 24−144), BRD3 BD2 (residues 306−417), BRD4 BD1 (residues 44−168), and BRD4 BD2 (residues 333−460) recombinant proteins were used in the binding assays. A fluorescence polarization (FP) binding assay was used to determine the binding affinities of the BET inhibitors to BRD2 (BD1 and BD2), BRD3 (BD1 and BD2), and BRD4 (BD1 and BD2) proteins, as described previously.[26,27]

Cell Growth Inhibition, Apoptosis Analysis, and Western Blotting. RS4;11 (CRL-1873) and MV4;11 (CRL-9591) human acute leukemia cell lines were purchased from the American Type Culture Collection. The MOLM13 (ACC554) human acute leukemia cell line was purchased from the DSMZ German cell bank. All the experiments were performed within two months of thawing fresh vials of the cells. RPMI-1640 and MV4;11 cells were cultured in IMDM media supplemented with 10% FBS and 50 U/mL penicillin−50 μg/mL streptomycin. Cells were maintained at 37 °C in a humidified atmosphere containing 5% CO_2 in air.

For cell growth experiments, compounds were diluted in the corresponding medium and then 3-fold serially diluted in a 96-well tissue culture plate to a final volume of 100 μL/well. Twenty thousand cells/well in 100 μL were added to each well containing compound to a final volume of 200 μL/well. Cells were incubated for 4 days at 37 °C in an atmosphere of 5% CO_2. Cell growth was evaluated utilizing a lactate dehydrogenase-based WST-8 assay (Dojindo Molecular Technologies, MD). An adequate volume of WST-8 reagent was added to each well, incubated for at least 1 h in the cell culture incubator, and read at 450 nm in a Tecan Infinite M1000 multimode microplate reader (Tecan, Morrisville, NC). The readings were normalized to the DMSO-treated cells and fitted using a nonlinear regression analysis with the GraphPad Prism 6 software to obtain the IC_{50} value for each compound.

Apoptosis induced by the BET degrader (**35**) and BET inhibitor (**22**) was evaluated using flow cytometry. Cells were treated with compounds at indicated concentrations for 24 or 48 h, collected, washed with cold PBS, and stained with Annexin V Alexa Fluor 488 and propidium iodide (PI) following manufacturer's instructions (ThermoFisher Scientific, CA). Stained cells were analyzed in the Attune NxT Flow Cytometer (ThermoFisher Scientific).

For Western blot analysis, 1.5−2 × 10^6 cells/well were plated in 12-well plates and treated with compounds at the indicated concentrations and times. Cells were collected, washed with cold PBS, and lysed in cold RIPA buffer containing Halt protease inhibitors. Twenty micrograms of lysate were run in each lane of 4−20% or 4−12% Novex gels and blotted into polyvinylidene difluoride membranes. Antibodies for immunoblotting were rabbit polyclonal antibodies for BRD2 (A302−583A), BRD3 (A302−368A), and BRD4 (A301−985A100) purchased from Bethyl Laboratories (Montgomery, TX,); c-Myc (D84C12), cleaved PARP (D64E10), and cleaved Caspase 3 (D3E9) from Cell Signaling Technology (Danvers, MA); GSPT1 polyclonal antibody (ab126090) from Abcam (Cambridge, MA); and HRP-GAPDH from Santa Cruz Biotechnology (Dallas, TX). The BIO-RAD Clarity

DOI: 10.1021/acs.jmedchem.8b00506
J. Med. Chem. XXXX, XXX, XXX−XXX

Western Enhanced Chemiluminescence Substrate was used for signal development. Blots were imaged in an iBright Imaging System (ThermoFisher).

Efficacy and Pharmacodynamics Studies in the RS4;11 and MV4;11 Xenograft Models in Mice. All animal experiments were performed under the guidelines of the University of Michigan Committee for Use and Care of Animals and using an approved animal protocol (PI, Shaomeng Wang).

Xenograft tumors were established by injecting 5×10^6 RS4;11 or MV4;11 cells in 50% Matrigel subcutaneously on the dorsal side of severe combined immunodeficient (SCID) mice, obtained from Charles River, one tumor per mouse. When tumors reached ∼100 mm^3, mice were randomly assigned to treatment and vehicle control groups. Animals were monitored daily for any signs of toxicity and weighed 2−3 times per week during the treatment period and at least weekly after the treatment ended. Tumor size was measured utilizing electronic calipers 2−3 times per week during the treatment period and at least weekly after the treatment ended. Tumor volume was calculated as $V = L \times W^2/2$, where L is the length and W is the width of the tumor.

For pharmacodynamic analysis, resected control and treated RS4;11 xenograft tumor tissues were ground into powder in liquid nitrogen and lysed in CST lysis buffer with halt proteinase inhibitors. Twenty micrograms of whole tumor clarified lysates were separated on 4−20% or 4−12% Novex gels. Western blots were performed as detailed in the previous section.

Methods for Tissue Distribution Study in RS4;11 Tumor-Bearing Mice. Female SCID mice bearing RS4;11 xenograft tumors were dosed with a single intravenous dose of compound **35** (QCA570) at 5 mg/kg. QCA570 was dissolved in the vehicle containing 20% (v/v) PEG400, 6% (v/v) CremophorEL and 74% (v/v) phosphate-buffered saline (PBS). The dosed animals were sacrificed at 1, 3, and 6 h for collecting different tissue and plasma samples. Isolated RS4;11 tumor samples, small intestinal, kidney, liver, heart, and lung were immediately frozen and placed in tared Precellys 2 mL hard tissue tubes with homogenizing ceramic beads 16859 (Cayman Chemical, Ann Arbor, MI), weighed, then stored at −80 °C for homogenization and analysis. Blood samples (400 μL) from each SCID mice were collected in 1.5 mL microfuge tubes containing heparin and centrifuged at 15000 rpm for 10 min. Then the plasmas were also stored at −80 °C until analysis.

To precipitate the proteins in mice plasma, 160 μL of acetonitrile containing 50 ng/mL of an internal standard was added to 40 μL of mouse plasma samples and vortexed for 10 min. The extracts were centrifuged at 15000 rpm, and the supernatant was transferred to the autosampler vials for LC−MS/MS analysis. Blank mouse plasma was used to prepare spiked calibration standards. The concentrations of the calibration standards were 2, 10, 50, 100, 250, 500, and 2000 ng/mL. Tumor and different tissue samples were homogenized by Precellys tissue homogenizer with the addition of a diluent solution, with a ratio of 5:1 (volume to 20% acetonitrile in water) (mL) to weight of tissue (g). Then the homogenized tissue solution was treated using the same procedure as that for the plasma samples to extract the compound for LC−MS/MS analysis.

Plasma and tissue concentrations of the compound were determined by the LC−MS/MS method developed and validated for this study. The LC−MS/MS method consisted of a Shimadzu LC-20AD HPLC system (Kyoto, Japan), and chromatographic separation of the tested compound was achieved using a Waters XBridageTM C18 column (50 × 2.1 mm, 3.5 μm) at 25 °C. Five microliters of the supernatant was injected. The flow rate of gradient elution was 0.4 mL/min with mobile phase A (0.1% formic acid in water) and mobile phase B (0.1% formic acid in acetonitrile). An AB Sciex QTrap 5500 mass spectrometer equipped with an electrospray ionization source (ABI-Sciex, Toronto, Canada) in the positive-ion multiple reaction monitoring (MRM) mode was used for detection. Protonated molecular ions and its respective ion products were monitored at the transitions of m/z 696.2 > 678.2 for QCA570 and 455.2 > 425.2 for the internal standard. We adjusted the instrument settings to maximize analytical sensitivity and specificity of detection. Total analysis time per sample was 5.7 min. Data were processed with software Analyst (version 1.6).

■ ASSOCIATED CONTENT

Supporting Information

The Supporting Information is available free of charge on the ACS Publications website at DOI: 10.1021/acs.jmedchem.8b00506.

Western blotting analysis of BRD2, BRD3, and BRD4 proteins in RS4;11 cells treated with BET inhibitor **22**, compound **26** and BET degraders **27**, **28**, **29**, **30**, and **31**; ^{1}H NMR spectrum of compound **35**; Western blotting analysis of GSPT1 protein in RS4;11 and MV4;11 cells treated with BET inhibitor **22** and BET degrader **35** (QCA570); ^{1}H NMR and ^{13}C NMR spectra and UPLC−MS chromatogram of compound **35** (PDF)

PDB coordinates of computational models of compounds **2** (PDB), **3** (PDB), and **22** (QCA276; PDB) in a complex with BRD4 BD1

Molecular string files for all the final target compounds (CSV)

■ AUTHOR INFORMATION

Corresponding Author

*E-mail: shaomeng@umich.edu.

ORCID

Bing Zhou: 0000-0003-1813-8035

Shaomeng Wang: 0000-0002-8782-6950

Present Address

○Department of Medicinal Chemistry, Shanghai Institute of Materia Medica, Chinese Academy of Sciences, Shanghai 201203, China.

Author Contributions

◆These authors contributed equally.

Notes

The authors declare the following competing financial interest(s): The University of Michigan has filed a number of patent applications on these BET inhibitors and degraders reported in this study, which have been licensed to Oncopia Therapeutics, LLC. S. Wang, H. Yang, Q. Chong, B. Zhou, C.-Y. Yang, F. Xu, J. Hu, Z. Chen, E. Fernandez-Salas, L. Bai, and D. McEachern are co-inventors on one or more of these patents and receive royalties on these patents from the University of Michigan. S. Wang is a co-founder and paid consultant of Oncopia Therapeutics, LLC, and owns stock in Oncopia.

■ ACKNOWLEDGMENTS

We are grateful for the financial support from the Breast Cancer Research Foundation (to S.W.), the Prostate Cancer Foundation (to S.W.), the National Cancer Institute, NIH (R01CA215758 to S.W.), and the University of Michigan Comprehensive Cancer Center support grant from the National Cancer Institute, NIH (P30 CA046592).

■ ABBREVIATIONS USED

BD1, BD2, bromodomain 1 and 2; BRD2, bromodomain-containing protein 2; BRD3, bromodomain-containing protein 3; BRD4, bromodomain-containing protein 4; HIV, human immunodeficiency virus; CNS, central nervous system; WPF, Trp81, Pro82, and Phe83; PARP, poly ADP ribose polymerase; FP, fluorescence polarization; GAPDH, glyceraldehyde 3-phosphate dehydrogenase; PD, pharmacodynamics; GSPT1, G1 to S phase transition 1; PROTAC, proteolysis targeting

DOI: 10.1021/acs.jmedchem.8b00506
J. Med. Chem. XXXX, XXX, XXX−XXX

chimera; SCID mice, severe combined immunodeficiency mice; TBDPS, *tert*-butyldiphenylsilyl

REFERENCES

(1) Tamkun, J. W.; Deuring, R.; Scott, M. P.; Kissinger, M.; Pattatucci, A. M.; Kaufman, T. C.; Kennison, J. A. Brahma: A Regulator of Drosophila Homeotic Genes Structurally Related to the Yeast Transcriptional Activator SNF2/SWl2. *Cell* **1992**, *68*, 561−572.

(2) Dhalluin, C.; Carlson, J. E.; Zeng, L.; He, C.; Aggarwal, A. K.; Zhou, M. M. Structure and Ligand of a Histone Acetyltransferase Bromodomain. *Nature* **1999**, *399*, 491−496.

(3) Patel, D. J.; Wang, Z. Readout of Epigenetic Modifications. *Annu. Rev. Biochem.* **2013**, *82*, 81−118.

(4) Belkina, A. C.; Denis, G. V. BET Domain Co-regulators in Obesity, Inflammation and Cancer. *Nat. Rev. Cancer* **2012**, *12*, 465−477.

(5) Arrowsmith, C. H.; Bountra, C.; Fish, P. V.; Lee, K.; Schapira, M. Epigenetic Protein Families: A New Frontier for Drug Discovery. *Nat. Rev. Drug Discovery* **2012**, *11*, 384−400.

(6) Chaidos, A.; Caputo, V.; Karadimitris, A. Inhibition of Bromodomain and Extra-Terminal Proteins (BET) as a Potential Therapeutic Approach in Haematological Malignancies: Emerging Preclinical and Clinical Evidence. *Ther. Adv. Hematol.* **2015**, *6*, 128−141.

(7) Xiao, Y.; Liang, L.; Huang, M.; Qiu, Q.; Zeng, S.; Shi, M.; Zou, Y.; Ye, Y.; Yang, X.; Xu, H. Bromodomain and Extra-Terminal Domain Bromodomain Inhibition Prevents Synovial Inflammation via Blocking IκB Kinase−Dependent NF-κB Activation in Rheumatoid Fibroblast-like Synoviocytes. *Rheumatology* **2016**, *55*, 173−184.

(8) Banerjee, C.; Archin, N.; Michaels, D.; Belkina, A. C.; Denis, G. V.; Bradner, J.; Sebastiani, P.; Margolis, D. M.; Montano, M. BET Bromodomain Inhibition as a Novel Strategy for Reactivation of HIV-1. *J. Leukocyte Biol.* **2012**, *92*, 1147−1154.

(9) Magistri, M.; Velmeshev, D.; Makhmutova, M.; Patel, P.; Sartor, G. C.; Volmar, C.-H.; Wahlestedt, C.; Ali Faghihi, M. The BET-Bromodomain Inhibitor JQ1 Reduces Inflammation and Tau Phosphorylation at Ser396 in the Brain of the 3xTg Model of Alzheimer's Disease. *Curr. Alzheimer Res.* **2016**, *13*, 985−995.

(10) Matzuk, M. M.; McKeown, M. R.; Filippakopoulos, P.; Li, Q.; Ma, L.; Agno, J. E.; Lemieux, M. E.; Picaud, S.; Yu, R. N.; Qi, J.; Knapp, S.; Bradner, J. E. Small-Molecule Inhibition of BRDT for Male Contraception. *Cell* **2012**, *150*, 673−684.

(11) Filippakopoulos, P.; Qi, J.; Picaud, S.; Shen, Y.; Smith, W. B.; Fedorov, O.; Morse, E. M.; Keates, T.; Hickman, T. T.; Felletar, I.; Philpott, M.; Munro, S.; McKeown, M. R.; Wang, Y.; Christie, A. L.; West, N.; Cameron, M. J.; Schwartz, B.; Heightman, T. D.; La Thangue, N.; French, C. A.; Wiest, O.; Kung, A. L.; Knapp, S.; Bradner, J. E. Selective Inhibition of BET Bromodomains. *Nature* **2010**, *468*, 1067−1073.

(12) Nicodeme, E.; Jeffrey, K. L.; Schaefer, U.; Beinke, S.; Dewell, S.; Chung, C. W.; Chandwani, R.; Marazzi, I.; Wilson, P.; Coste, H.; White, J.; Kirilovsky, J.; Rice, C. M.; Lora, J. M.; Prinjha, R. K.; Lee, K.; Tarakhovsky, A. Suppression of Inflammation by a Synthetic Histone Mimic. *Nature* **2010**, *468*, 1119−1123.

(13) Dawson, M. A.; Prinjha, R. K.; Dittmann, A.; Giotopoulos, G.; Bantscheff, M.; Chan, W. I.; Robson, S. C.; Chung, C. W.; Hopf, C.; Savitski, M. M.; Huthmacher, C.; Gudgin, E.; Lugo, D.; Beinke, S.; Chapman, T. D.; Roberts, E. J.; Soden, P. E.; Auger, K. R.; Mirguet, O.; Doehner, K.; Delwel, R.; Burnett, A. K.; Jeffrey, P.; Drewes, G.; Lee, K.; Huntly, B. J.; Kouzarides, T. Inhibition of BET Recruitment to Chromatin as an Effective Treatment for MLL-Fusion Leukaemia. *Nature* **2011**, *478*, 529−533.

(14) Filippakopoulos, P.; Knapp, S. Targeting Bromodomains: Epigenetic Readers of Lysine Ccetylation. *Nat. Rev. Drug Discovery* **2014**, *13*, 337−356.

(15) Chung, C. W.; Coste, H.; White, J. H.; Mirguet, O.; Wilde, J.; Gosmini, R. L.; Delves, C.; Magny, S. M.; Woodward, R.; Hughes, S. A.; Boursier, E. V.; Flynn, H.; Bouillot, A. M.; Bamborough, P.; Brusq, J. M.; Gellibert, F. J.; Jones, E. J.; Riou, A. M.; Homes, P.; Martin, S. L.; Uings, I. J.; Toum, J.; Clement, C. A.; Boullay, A. B.; Grimley, R. L.; Blandel, F. M.; Prinjha, R. K.; Lee, K.; Kirilovsky, J.; Nicodeme, E. Discovery and Characterization of Small Molecule Inhibitors of the BET Family Bromodomains. *J. Med. Chem.* **2011**, *54*, 3827−3838.

(16) Gehling, V. S.; Hewitt, M. C.; Vaswani, R. G.; Leblanc, Y.; Cote, A.; Nasveschuk, C. G.; Taylor, A. M.; Harmange, J. C.; Audia, J. E.; Pardo, E.; Joshi, S.; Sandy, P.; Mertz, J. A.; Sims, R. J., 3rd; Bergeron, L.; Bryant, B. M.; Bellon, S.; Poy, F.; Jayaram, H.; Sankaranarayanan, R.; Yellapantula, S.; Bangalore Srinivasamurthy, N.; Birudukota, S.; Albrecht, B. K. Discovery, Design, and Optimization of Isoxazole Azepine BET Inhibitors. *ACS Med. Chem. Lett.* **2013**, *4*, 835−840.

(17) Zhang, G.; Plotnikov, A. N.; Rusinova, E.; Shen, T.; Morohashi, K.; Joshua, J.; Zeng, L.; Mujtaba, S.; Ohlmeyer, M.; Zhou, M. M. Structure-guided Design of Potent Diazobenzene Inhibitors for the BET Bromodomains. *J. Med. Chem.* **2013**, *56*, 9251−9264.

(18) Taylor, A. M.; Vaswani, R. G.; Gehling, V. S.; Hewitt, M. C.; Leblanc, Y.; Audia, J. E.; Bellon, S.; Cummings, R. T.; Cote, A.; Harmange, J. C.; Jayaram, H.; Joshi, S.; Lora, J. M.; Mertz, J. A.; Neiss, A.; Pardo, E.; Nasveschuk, C. G.; Poy, F.; Sandy, P.; Setser, J. W.; Sims, R. J., 3rd; Tang, Y.; Albrecht, B. K. Discovery of Benzotriazolo[4,3-d][1,4]diazepines as Orally Active Inhibitors of BET Bromodomains. *ACS Med. Chem. Lett.* **2016**, *7*, 145−150.

(19) Xue, X.; Zhang, Y.; Liu, Z.; Song, M.; Xing, Y.; Xiang, Q.; Wang, Z.; Tu, Z.; Zhou, Y.; Ding, K.; Xu, Y. Discovery of Benzo[cd]indol-2(1H)-ones as Potent and Specific BET Bromodomain Inhibitors: Structure-Based Virtual Screening, Optimization, and Biological Evaluation. *J. Med. Chem.* **2016**, *59*, 1565−1579.

(20) Ayoub, A. M.; Hawk, L. M. L.; Herzig, R. J.; Jiang, J.; Wisniewski, A. J.; Gee, C. T.; Zhao, P.; Zhu, J. Y.; Berndt, N.; Offei-Addo, N. K.; Scott, T. G.; Qi, J.; Bradner, J. E.; Ward, T. R.; Schonbrunn, E.; Georg, G. I.; Pomerantz, W. C. K. BET Bromodomain Inhibitors with One-Step Synthesis Discovered from Virtual Screen. *J. Med. Chem.* **2017**, *60*, 4805−4817.

(21) Millan, D. S.; Kayser-Bricker, K. J.; Martin, M. W.; Talbot, A. C.; Schiller, S. E. R.; Herbertz, T.; Williams, G. L.; Luke, G. P.; Hubbs, S.; Alvarez Morales, M. A.; Cardillo, D.; Troccolo, P.; Mendes, R. L.; McKinnon, C. Design and Optimization of Benzopiperazines as Potent Inhibitors of BET Bromodomains. *ACS Med. Chem. Lett.* **2017**, *8*, 847−852.

(22) Sharp, P. P.; Garnier, J. M.; Hatfaludi, T.; Xu, Z.; Segal, D.; Jarman, K. E.; Jousset, H.; Garnham, A.; Feutrill, J. T.; Cuzzupe, A.; Hall, P.; Taylor, S.; Walkley, C. R.; Tyler, D.; Dawson, M. A.; Czabotar, P.; Wilks, A. F.; Glaser, S.; Huang, D. C. S.; Burns, C. J. Design, Synthesis, and Biological Activity of 1,2,3-Triazolobenzodiazepine BET Bromodomain Inhibitors. *ACS Med. Chem. Lett.* **2017**, *8*, 1298−1303.

(23) Wang, L.; Pratt, J. K.; Soltwedel, T.; Sheppard, G. S.; Fidanze, S. D.; Liu, D.; Hasvold, L. A.; Mantei, R. A.; Holms, J. H.; McClellan, W. J.; Wendt, M. D.; Wada, C.; Frey, R.; Hansen, T. M.; Hubbard, R.; Park, C. H.; Li, L.; Magoc, T. J.; Albert, D. H.; Lin, X.; Warder, S. E.; Kovar, P.; Huang, X.; Wilcox, D.; Wang, R.; Rajaraman, G.; Petros, A. M.; Hutchins, C. W.; Panchal, S. C.; Sun, C.; Elmore, S. W.; Shen, Y.; Kati, W. M.; McDaniel, K. F. Fragment-Based, Structure-Enabled Discovery of Novel Pyridones and Pyridone Macrocycles as Potent Bromodomain and Extra-Terminal Domain (BET) Family Bromodomain Inhibitors. *J. Med. Chem.* **2017**, *60*, 3828−3850.

(24) Law, R. P.; Atkinson, S. J.; Bamborough, P.; Chung, C. W.; Demont, E. H.; Gordon, L. J.; Lindon, M.; Prinjha, R. K.; Watson, A. J. B.; Hirst, D. J. Discovery of Tetrahydroquinoxalines as Bromodomain and Extra-Terminal Domain (BET) Inhibitors with Selectivity for the Second Bromodomain. *J. Med. Chem.* **2018**, *61*, 4317−4334.

(25) Zhang, M.; Zhang, Y.; Song, M.; Xue, X.; Wang, J.; Wang, C.; Zhang, C.; Li, C.; Xiang, Q.; Zou, L.; Wu, X.; Wu, C.; Dong, B.; Xue, W.; Zhou, Y.; Chen, H.; Wu, D.; Ding, K.; Xu, Y. Structure-Based Discovery and Optimization of Benzo[d]isoxazole Derivatives as Potent and Selective BET Inhibitors for Potential Treatment of Castration-Resistant Prostate Cancer (CRPC). *J. Med. Chem.* **2018**, *61*, 3037−3058.

(26) Zhao, Y.; Bai, L.; Liu, L.; McEachern, D.; Stuckey, J. A.; Meagher, J. L.; Yang, C. Y.; Ran, X.; Zhou, B.; Hu, Y.; Li, X.; Wen, B.; Zhao, T.; Li,

DOI: 10.1021/acs.jmedchem.8b00506
J. Med. Chem. XXXX, XXX, XXX−XXX

S.; Sun, D.; Wang, S. Structure-Based Discovery of 4-(6-Methoxy-2-methyl-4-(quinolin-4-yl)-9H-pyrimido[4,5-b]indol-7-yl)-3,5-dimethylisoxazole (CD161) as a Potent and Orally Bioavailable BET Bromodomain Inhibitor. *J. Med. Chem.* **2017**, *60*, 3887−3901.
(27) Ran, X.; Zhao, Y.; Liu, L.; Bai, L.; Yang, C.-Y.; Zhou, B.; Meagher, J. L.; Chinnaswamy, K.; Stuckey, J. A.; Wang, S. Structure-based Design of γ-Carboline Analogues as Potent and Specific BET Bromodomain Inhibitors. *J. Med. Chem.* **2015**, *58*, 4927−4939.
(28) Coudé, M.-M.; Braun, T.; Berrou, J.; Dupont, M.; Bertrand, S.; Masse, A.; Raffoux, E.; Itzykson, R.; Delord, M.; Riveiro, M. E. BET Inhibitor OTX015 Targets BRD2 and BRD4 and Decreases c-MYC in Acute Leukemia Cells. *Oncotarget* **2015**, *6*, 17698−17712.
(29) Smith, S. G.; Sanchez, R.; Zhou, M. M. Privileged Diazepine Compounds and Their Emergence as Bromodomain Inhibitors. *Chem. Biol.* **2014**, *21*, 573−583.
(30) Sakamoto, K. M.; Kim, K. B.; Kumagai, A.; Mercurio, F.; Crews, C. M.; Deshaies, R. J. Protacs: Chimeric Molecules that Target Proteins to the Skp1-Cullin-F box Complex for Ubiquitination and Degradation. *Proc. Natl. Acad. Sci. U. S. A.* **2001**, *98*, 8554−8559.
(31) Raina, K.; Crews, C. M. Chemical Inducers of Targeted Protein Degradation. *J. Biol. Chem.* **2010**, *285*, 11057−11060.
(32) Tinworth, C. P.; Lithgow, H.; Churcher, I. Small Molecule-mediated Protein Knockdown as a New Approach to Drug Discovery. *MedChemComm* **2016**, *7*, 2206−2216.
(33) Toure, M.; Crews, C. M. Small-Molecule PROTACS: New Approaches to Protein Degradation. *Angew. Chem., Int. Ed.* **2016**, *55*, 1966−1973.
(34) Ottis, P.; Crews, C. M. Proteolysis-Targeting Chimeras: Induced Protein Degradation as a Therapeutic Strategy. *ACS Chem. Biol.* **2017**, *12*, 892−898.
(35) Salami, J.; Crews, C. M. Waste Disposal-An Attractive Strategy for Cancer Therapy. *Science* **2017**, *355*, 1163−1167.
(36) Walczak, M. J.; Petzold, G.; Thoma, N. H. Targeted Protein Degradation: You Can Glue It Too! *Nat. Chem. Biol.* **2017**, *13*, 452−453.
(37) Gustafson, J. L.; Neklesa, T. K.; Cox, C. S.; Roth, A. G.; Buckley, D. L.; Tae, H. S.; Sundberg, T. B.; Stagg, D. B.; Hines, J.; McDonnell, D. P.; Norris, J. D.; Crews, C. M. Small-Molecule-Mediated Degradation of the Androgen Receptor through Hydrophobic Tagging. *Angew. Chem., Int. Ed.* **2015**, *54*, 9659−9662.
(38) Cyrus, K.; Wehenkel, M.; Choi, E. Y.; Lee, H.; Swanson, H.; Kim, K. B. Jostling for Position: Optimizing Linker Location in the Design of Estrogen Receptor-Targeting PROTACs. *ChemMedChem* **2010**, *5*, 979−985.
(39) Demizu, Y.; Okuhira, K.; Motoi, H.; Ohno, A.; Shoda, T.; Fukuhara, K.; Okuda, H.; Naito, M.; Kurihara, M. Design and Synthesis of Estrogen Receptor Degradation Inducer Dased on a Protein Knockdown Strategy. *Bioorg. Med. Chem. Lett.* **2012**, *22*, 1793−1796.
(40) Bondeson, D. P.; Mares, A.; Smith, I. E.; Ko, E.; Campos, S.; Miah, A. H.; Mulholland, K. E.; Routly, N.; Buckley, D. L.; Gustafson, J. L.; Zinn, N.; Grandi, P.; Shimamura, S.; Bergamini, G.; Faelth-Savitski, M.; Bantscheff, M.; Cox, C.; Gordon, D. A.; Willard, R. R.; Flanagan, J. J.; Casillas, L. N.; Votta, B. J.; den Besten, W.; Famm, K.; Kruidenier, L.; Carter, P. S.; Harling, J. D.; Churcher, I.; Crews, C. M. Catalytic in vivo Protein Knockdown by Small-Molecule PROTACs. *Nat. Chem. Biol.* **2015**, *11*, 611−617.
(41) Demizu, Y.; Shibata, N.; Hattori, T.; Ohoka, N.; Motoi, H.; Misawa, T.; Shoda, T.; Naito, M.; Kurihara, M. Development of BCR-ABL Degradation Inducers via the Conjugation of an Imatinib Derivative and a cIAP1 Ligand. *Bioorg. Med. Chem. Lett.* **2016**, *26*, 4865−4869.
(42) Lai, A. C.; Toure, M.; Hellerschmied, D.; Salami, J.; Jaime-Figueroa, S.; Ko, E.; Hines, J.; Crews, C. M. Modular PROTAC Design for the Degradation of Oncogenic BCR-ABL. *Angew. Chem., Int. Ed.* **2016**, *55*, 807−810.
(43) Winter, G. E.; Buckley, D. L.; Paulk, J.; Roberts, J. M.; Souza, A.; Dhe-Paganon, S.; Bradner, J. E. Phthalimide Conjugation as a Strategy for in vivo Target Protein Degradation. *Science* **2015**, *348*, 1376−1381.
(44) Zhou, B.; Hu, J.; Xu, F.; Chen, Z.; Bai, L.; Fernandez-Salas, E.; Lin, M.; Liu, L.; Yang, C. Y.; Zhao, Y.; McEachern, D.; Przybranowski, S.; Wen, B.; Sun, D.; Wang, S. Discovery of a Small-Molecule Degrader of Bromodomain and Extra-Terminal (BET) Proteins with Picomolar Cellular Potencies and Capable of Achieving Tumor Regression. *J. Med. Chem.* **2018**, *61*, 462−481.
(45) Bai, L.; Zhou, B.; Yang, C. Y.; Ji, J.; McEachern, D.; Przybranowski, S.; Jiang, H.; Hu, J.; Xu, F.; Zhao, Y.; Liu, L.; Fernandez-Salas, E.; Xu, J.; Dou, Y.; Wen, B.; Sun, D.; Meagher, J.; Stuckey, J.; Hayes, D. F.; Li, S.; Ellis, M. J.; Wang, S. Targeted Degradation of BET Proteins in Triple-Negative Breast Cancer. *Cancer Res.* **2017**, *77*, 2476−2487.
(46) Winter, G. E.; Mayer, A.; Buckley, D. L.; Erb, M. A.; Roderick, J. E.; Vittori, S.; Reyes, J. M.; di Iulio, J.; Souza, A.; Ott, C. J.; Roberts, J. M.; Zeid, R.; Scott, T. G.; Paulk, J.; Lachance, K.; Olson, C. M.; Dastjerdi, S.; Bauer, S.; Lin, C. Y.; Gray, N. S.; Kelliher, M. A.; Churchman, L. S.; Bradner, J. E. BET Bromodomain Proteins Function as Master Transcription Elongation Factors Independent of CDK9 Recruitment. *Mol. Cell* **2017**, *67*, 5−18.
(47) Raina, K.; Lu, J.; Qian, Y.; Altieri, M.; Gordon, D.; Rossi, A. M.; Wang, J.; Chen, X.; Dong, H.; Siu, K.; Winkler, J. D.; Crew, A. P.; Crews, C. M.; Coleman, K. G. PROTAC-induced BET Protein Degradation as a Therapy for Castration-Resistant Prostate Cancer. *Proc. Natl. Acad. Sci. U. S. A.* **2016**, *113*, 7124−7129.
(48) Zengerle, M.; Chan, K. H.; Ciulli, A. Selective Small Molecule Induced Degradation of the BET Bromodomain Protein BRD4. *ACS Chem. Biol.* **2015**, *10*, 1770−1777.
(49) Lu, J.; Qian, Y.; Altieri, M.; Dong, H.; Wang, J.; Raina, K.; Hines, J.; Winkler, J. D.; Crew, A. P.; Coleman, K.; Crews, C. M. Hijacking the E3 Ubiquitin Ligase Cereblon to Efficiently Target BRD4. *Chem. Biol.* **2015**, *22*, 755−763.
(50) Picaud, S.; Wells, C.; Felletar, I.; Brotherton, D.; Martin, S.; Savitsky, P.; Diez-Dacal, B.; Philpott, M.; Bountra, C.; Lingard, H.; Fedorov, O.; Muller, S.; Brennan, P. E.; Knapp, S.; Filippakopoulos, P. RVX-208, an Inhibitor of BET Transcriptional Regulators with Selectivity for the Second Bromodomain. *Proc. Natl. Acad. Sci. U. S. A.* **2013**, *110*, 19754−19759.
(51) Ito, T.; Ando, H.; Suzuki, T.; Ogura, T.; Hotta, K.; Imamura, Y.; Yamaguchi, Y.; Handa, H. Identification of a Primary Target of Thalidomide Teratogenicity. *Science* **2010**, *327*, 1345−1350.
(52) Fischer, E. S.; Böhm, K.; Lydeard, J. R.; Yang, H.; Stadler, M. B.; Cavadini, S.; Nagel, J.; Serluca, F.; Acker, V.; Lingaraju, G. M. Structure of the DDB1−CRBN E3 Ubiquitin Ligase in Complex with Thalidomide. *Nature* **2014**, *512*, 49−53.
(53) Chamberlain, P. P.; Lopez-Girona, A.; Miller, K.; Carmel, G.; Pagarigan, B.; Chie-Leon, B.; Rychak, E.; Corral, L. G.; Ren, Y. J.; Wang, M. Structure of the Human Cereblon−DDB1−Lenalidomide Complex Reveals Basis for Responsiveness to Thalidomide Analogs. *Nat. Struct. Mol. Biol.* **2014**, *21*, 803−809.
(54) Delmore, J. E.; Issa, G. C.; Lemieux, M. E.; Rahl, P. B.; Shi, J.; Jacobs, H. M.; Kastritis, E.; Gilpatrick, T.; Paranal, R. M.; Qi, J.; Chesi, M.; Schinzel, A. C.; McKeown, M. R.; Heffernan, T. P.; Vakoc, C. R.; Bergsagel, P. L.; Ghobrial, I. M.; Richardson, P. G.; Young, R. A.; Hahn, W. C.; Anderson, K. C.; Kung, A. L.; Bradner, J. E.; Mitsiades, C. S. BET Bromodomain Inhibition as a Therapeutic Strategy to Target c-Myc. *Cell* **2011**, *146*, 904−917.
(55) Matyskiela, M. E.; Lu, G.; Ito, T.; Pagarigan, B.; Lu, C. C.; Miller, K.; Fang, W.; Wang, N. Y.; Nguyen, D.; Houston, J.; Carmel, G.; Tran, T.; Riley, M.; Nosaka, L.; Lander, G. C.; Gaidarova, S.; Xu, S.; Ruchelman, A. L.; Handa, H.; Carmichael, J.; Daniel, T. O.; Cathers, B. E.; Lopez-Girona, A.; Chamberlain, P. P. A Novel Cereblon Modulator Recruits GSPT1 to the CRL4(CRBN) Ibiquitin Ligase. *Nature* **2016**, *535*, 252−257.
(56) *MOE*; Chemical Computing Group: Montreal, Quebec, Canada.
(57) Jones, G.; Willett, P.; Glen, R. C.; Leach, A. R.; Taylor, R. Development and Validation of a Genetic Algorithm for Flexible Docking. *J. Mol. Biol.* **1997**, *267*, 727−748.

DOI: 10.1021/acs.jmedchem.8b00506
J. Med. Chem. XXXX, XXX, XXX−XXX

(58) Verdonk, M. L.; Cole, J. C.; Hartshorn, M. J.; Murray, C. W.; Taylor, R. D. Improved Protein-Ligand Docking Using GOLD. *Proteins: Struct., Funct., Genet.* **2003**, *52*, 609−623.

DOI: 10.1021/acs.jmedchem.8b00506
J. Med. Chem. XXXX, XXX, XXX−XXX